DOI: 10.1161/CIRCULATIONAHA.114.014822

Pentraxin 3 Induces Vascular Endothelial Dysfunction Through a P-selectin/MMP-1 Pathway

Running title: *Carrizzo et al.; PTX3 induces endothelial dysfunction*

Albino Carrizzo, MSc[1]; Paola Lenzi, PhD[2]; Claudio Procaccini, PhD[3]; Antonio Damato, BSc[1]; Francesca Biagioni, PhD[1]; Ambrosio Mariateresa, BSc[1]; Giusy Amodio, PhD[4,5]; Paolo Remondelli, PhD[5]; Carmine Del Giudice, MSc[6]; Raffaele Izzo, MD[6]; Alberto Malovini, PhD[7]; Luigi Formisano, PhD[8]; Vincenzo Gigantino, MSc[3,9]; Michele Madonna, DVM, PhD[1]; Annibale A. Puca, MD[5,10]; Bruno Trimarco, MD[6]; Giuseppe Matarese, MD[5,10], Francesco Fornai, PhD, MD[1,2], Carmine Vecchione, MD[1,5]

[1]IRCCS Neuromed, Pozzilli (IS), Italy; [2]Dept of Human Morphology and Applied Biology, University of Pisa, Pisa, Italy; [3]Laboratorio di Immunologia, Istituto di Endocrinologia e Oncologia Sperimentale, (IEOS-CNR), Consiglio Nazionale delle Ricerche c/o Dipartimento di Medicina Molecolare e Biotecnologie Mediche, Università di Napoli "Federico II", Napoli, Italy; [4]Dept of Pharmaceutical Sciences,Università degli Studi di Salerno, Fisciano (Salerno), Italy; [5]Medicine and Surgery, Università degli Studi di Salerno, Baronissi (Salerno), Italy; [6]Dept of Clinical Medicine, Cardiovascular and Immunological Sciences, "Federico II" University of Naples, Italy; [7]Dept of Industrial and Information Engineering, University of Pavia, Pavia, Italy; [8]Dept of Science and Technology, University of Sannio, Benevento, Italy; [9]Pathology Unit, "Istituto Nazionale Tumori, IRCCS, Fondazione Pascale", Naples, Italy; [10]IRCCS Multimedica, Milan, Italy

Address for Correspondence:

Carmine Vecchione, MD

Department of Medicine and Surgery

University of Salerno; IRCCS Neuromed

Via Allende, Loc. Camerelle

Salerno, 86077 Italy

Tel: +39 08 6591 5229

Fax: +39 08 6592 7575

E-mail: cvecchione@unisa.it

Journal Subject Codes: Vascular biology:[97] Other vascular biology, Hypertension:[14] Other hypertension

DOI: 10.1161/CIRCULATIONAHA.114.014822

Abstract

***Background*—**Pentraxin 3 (PTX3), the prototype of long pentraxins, has been described associated with endothelial dysfunction in different cardiovascular disorders. So far, no study has evaluated the possible direct effect of PTX3 on vascular function.

***Methods and Results*—**Through in-vitro experiments of vascular reactivity and ultrastructural analyses, we demonstrate that PTX3 induces, *per se*, dysfunction and morphological changes of the endothelial layer through a P-selectin/metalloproteinase-1 (MMP1) pathway. The latter hampered the detachment of eNOS from Caveolin1, leading to an impairment of nitric oxide (NO) signaling. In vivo studies showed that the administration of PTX3 to wild-type mice induced endothelial dysfunction and increased blood pressure, an effect absent in P-selectin-deficient mice. In isolated endothelial cells (HUVEC), PTX3 significantly blunted NO production through the MMP1 pathway. Finally, using ELISA, we found that hypertensive patients (n=31) have higher plasma levels of PTX3 and its mediators P-Selectin and MMP1 than normotensive subjects (n=21).

***Conclusions*—**Our data show for the first time a direct role of PTX3 on vascular function and blood pressure homeostasis, identifying the molecular mechanisms involved. The findings in humans suggest that PTX3, P-selectin and MMP-1 may be novel biomarkers that predict the onset of vascular dysfunction in hypertensive patients.

Key words: endothelial dysfunction, vascular biology, biomarker

DOI: 10.1161/CIRCULATIONAHA.114.014822

Introduction

The pentraxin (PTX) family includes two subgroups of proteins that are structurally divided into short and long forms and that are encoded by different genes and produced by different cells[1-3]. PTX3 is the prototype of the long PTX group, which differs from short PTXs by the presence of an unrelated long N-terminal domain giving it a different ligand recognition capacity [4]. PTX3 is highly conserved from mouse to humans (82% identical and 92% conserved amino acids) and is induced by primary inflammatory stimuli in a variety of cell types[5, 6], including mononuclear phagocytes, fibroblasts, adipocytes, dendritic, endothelial and smooth muscle cells[5, 7]. Marked as an innate immunity protein, PTX3 regulates not only inflammatory responses but is involved in a range of important biological mechanisms, including vascular pathology. In fact, blood vessels produce large amounts of PTX3 during inflammation, and the level of circulating PTX3 increases in several pathological conditions affecting the cardiovascular system[8, 9]. Moreover, in advanced atherosclerotic lesions and in patients with vasculitis, the protein is abundantly present in endothelial cells[10, 11]. Thus, PTX3 seems to be a rapid marker of primary local innate immunity and inflammation activation, and a novel diagnostic tool for vascular disorders.

In addition, high plasma PTX3 has been linked with vascular endothelial dysfunction in several human diseases, including chronic kidney disease and preeclampsia, a multisystemic disorder associated with hypertension[12-14]. Endothelial dysfunction is considered to be an early pathophysiological feature of hypertension, which is strictly associated with increased inflammatory and adhesion molecules in the vascular wall[8]. So far, no studies have reported a possible direct role of inflammatory molecules, such as PTX3, on vascular homeostasis or possible involvement in modulation of endothelial function.

Here, we demonstrate that: 1) PTX3 induces, *per se*, vascular dysfunction and

morphological changes of the endothelial layer in experimental models via an adhesion molecule P-selectin/MMP1 pathway that converges on nitric oxide signaling; 2) in vivo PTX3 induces endothelial dysfunction and increases blood pressure in mice; 3) PTX3 impairs NO production through the MMP1 pathway in HUVEC; and 4) PTX3 and its mediators of vascular damage, P-selectin and MMP-1, are elevated in plasma of hypertensive patients:

Methods

For detailed methodology, please see the Online Data Supplement. In brief, we performed vascular reactivity studies on resistance vessels from C57BL6 mice and from FCγR- and P-selectin-knock-out mice to evaluate PTX3 *in-vitro* vascular effects. To test the *in-vivo* effect of PTX3 on blood pressure in mice, we used a polyethylene catheter inserted into a femoral artery. After vascular reactivity, proteins were rapidly extracted from vessels to perform immunoprecipitation and immunoblot studies. Low temperature SDS-PAGE was used to evaluate ratio of eNOS dimer and monomer. Morphological analyses and ultrastructural evaluation of CAV-1 or MMP-1 localization in mesenteric arteries were performed using Transmission Electron Microscopy (TEM). Macroscopic alterations on mesenteric arteries were evaluated using evans blue dye method. Human Umbilical Vein Endothelial Cells (HUVEC) were used to measured MMP1 activity through the SensoLyte® Plus 520 MMP-1 Assay Kit *Fluorimetric and Enhanced Selectivity* (Anaspec); NO production was measured using Sievers 280i NO Analyzer; P-selectin/PTX3 colocalization was evaluated using the immunofluorescence analysis, and P-selectin expression was evaluated through flow cytometric analysis. Finally, plasma levels of PTX3, P-selectin and MMP-1 in hypertensive and normotensive subjects were measured using a high-sensitivity, enzyme-linked immunosorbent assay (ELISA) system for

human plasma. The study was approved by an institutional review committee and the subjects gave their informed consent.

Statistical analyses

All statistical analyses were performed with Prism (GraphPad). Two-tailed Student's *t* test was used to calculate statistical significance of western blot experiments. Data from all experiments are given as means ± standard deviation (SD), except for the vascular reactivity experiments for which data are given as means ± standard error of mean (SEM). Analysis of Mean arterial pressure and vascular reactivity curves were performed using the non-parametric test of Mann-Whitney. *P*-value <0.05 was considered to be significant. The Shapiro-Wilk test was used to evaluate potential deviations of the analysed quantitative variables of ELISA values from the normal distribution ($p < 0.05$). Quantitative variables following the normal distribution were described by mean ± standard deviation (SD) or by median (25th – 75th percentiles) otherwise. The Welch's t-test was applied to test for statistically significant difference in terms of normally distributed variables between hypertensive and control subjects. The Wilcoxon rank-sum test was used to test for statistically significant difference in terms of quantitative variables deviating from the normal distribution between hypertensive and control subjects. The *roc* function implemented in the R package called *pROC* was used to estimate the Area Under the Receiver Operating Characteristic curves (AUROC) and corresponding 95% Confidence Interval (95% CI) for each variable. The response variable of each model was represented by the hypertensive/control condition, while the predictor variables were: PTX3, SELP or MMP-1 raw measures. ROC curves were compared by the *roc test* function implemented in the R package called "pROC". In order to identify the most informative threshold for each variable to discriminate hypertensive subjects from controls, the dataset was randomly split into a training

set (70% of the whole sample) and a test set (30% of the data) with stratification, so that the proportion of cases and controls observed in the whole sample was maintained in the two sub-cohorts. Thus, the most informative thresholds were identified among all the possible values observed on the *training set* as the ones guaranteeing the highest Mattew's Correlation Coefficient (MCC), which is the most appropriate parameter for the analysis of datasets characterized by unbalanced outcomes. The discriminative performances of the analysed variables discretized according to the identified thresholds were assessed on the independent training and *test set* in terms of MCC, sensitivity (Sens.), specificity (Spec.), positive predictive value (PPV), negative predictive value (NPV) and F-Measure (F). Statistical tests were performed by the R software v. 3.1.0 (www.r-project.org/).

Results

PTX3 induces endothelial dysfunction in mouse resistance vessels.

Elevated levels of PTX3 have been associated with endothelial dysfunction in humans [12-15]. Therefore, we evaluated whether the protein was able, *per se*, to influence endothelial function, which is impaired in hypertension[16]. To this end, we tested the effects of increasing doses of PTX3 (2, 20 and 200 ng/mL) for different preincubation times (15, 30, 45 and 60 minutes) on acetylcholine-evoked endothelial vasorelaxation of preconstricted mouse mesenteric vessels (**Fig. 1**). We found that 2 ng PTX3/mL did not influence endothelial function (**Fig. 1a**). In contrast, 20 ng/mL induced a significant reduction in acetylcholine-evoked vasorelaxation after 45 minutes of preincubation; the effect was similar to that observed after 60 minutes (**Fig.1b**).The endothelial vasorelaxation observed in the presence of 200ng PTX3/mL (**Fig.1c**) was not statistically different from that evoked by 20 ng/mL. Thus, we decided to use 20 ng/mL

for 45 minutes of preincubation in all subsequent in vitro experiments.

To understand whether PTX3's vascular action on the endothelium was generalized or specific for a vascular district, we tested its effect on other vascular beds, such as femoral arteries and aorta. PTX3 induced endothelial dysfunction of femoral artery (**Fig. S1a**) but not of windkessel, such us aorta (**Fig. S1b**). Moreover, the vascular action of PTX3 was specific for endothelial function, since nitroglycerine-evoked relaxation of smooth muscle was not influenced (data not shown).

Fluorescence immunostaining using exogenous biotinylated PTX3 clearly showed that the protein was endothelially localized, as evidenced by the specific interaction between biotin and fluorescent streptavidin (**Fig. 1d**). Of note, it was not observed in the aorta, in which PTX3 failed to exert any vascular effect (**Fig. S1c**). Taken together, these findings demonstrate that the target of PTX3's vascular action is the endothelium and that it induces dysfunction of resistance vessels.

P-selectin mediates PTX3's action on the endothelium.

In the immunology field, P-selectin and FcγR have been identified as two receptors of PTX3[17, 18], but there is no data on the involvement of such receptor(s) at the vascular level. To clarify this issue, we performed experiments on mesenteric arteries from P-selectin and FCγR-knockout mice, testing the endothelial vascular effect of PTX3. Vascular reactivity studies demonstrated that PTX3 blunted acetylcholine-evoked vasorelaxation in FCγR knockout vessels (**Fig. 2a**), but failed to exert any effect in P-selectin-deficient ones (**Fig. 2b**). These results indicated P-selectin as the cognate receptor of PTX3 in endothelial cells. In agreement, P-selectin immunoprecipitated with PTX3 in wild-type (WT) mesenteric artery lysates. As expected, P-selectin could not be immunoprecipitated from P-selectin-knockout mice (**Fig. 2c**).

In addition to PTX3, P-Selectin interacts also with Serum Amyloid Protein (SAP) in immunological[19] and vascular processes. We found that SAP-evoked endothelial dysfunction failed to exert an effect in P-selectin KO mice (**Fig**. **S2a**). This action is not common to other inflammatory factors such as C-reactive protein (CRP) that induce endothelial dysfunction through interaction with the FCgammaIIB receptor[20]. In agreement, CRP was still able to induce its vascular effect in P-selectin KO mice (**Fig. S2b**).

PTX3-evoked endothelial dysfunction is associated with morphological changes of endothelial cells.

An interesting observation emerging from vascular reactivity studies was that endothelial dysfunction was still present after continuous wash-out of PTX3 from the organ bath housing the vessels (**Fig. 3a**). This finding lead us to hypothesize that PTX3 induced a morphological alteration. We therefore studied mesenteric arteries at the ultrastructural level to see whether treatment with PTX3 could induce phenotypical alterations in vascular cells. WT vessels treated with vehicle had a normal architecture with typical indented nuclei, well-organized cytoplasm and intact plasma membrane (**Fig. 3b**, panel 1). In contrast, PTX3 induced the presence of large vacuoles, a diluted cytoplasm and a broken plasma membrane (**Fig. 3b**, panel 2). Of note, no structural alterations were detected in P-selectin$^{-/-}$ mesenteric endothelial cells after exposure to vehicle or PTX3 (**Fig. 3b**, panels 3 and 4); moreover, no structural changes were seen in the smooth muscle layer after exposure to PTX3 (data not shown). In agreement, Evans Blue Dye (EBD) staining, which identifies vascular leakage, was acquired only by PTX3-treated vessels (additional data in the Results section of the Online Data Supplement and **Figure S3**).

PTX3-induced vascular morphological changes are mediated by a P-selectin/metalloproteinase-1 pathway

Based on the results of the ultrastructural analysis of mesenteric arteries, we focused our attention to the identification of the mediators of the morphological alterations induced by PTX3, exploring the involvement of important molecules recruited in vascular structural changes, namely metalloproteinases (MMPs). We first evaluated the effect of PTX3 on endothelial function in the presence of GM6001, an inhibitor of MMP-1, -2, -3, -8 and -9. In agreement with our hypothesis, this non-selective MMP inhibitor protected mesenteric arteries from the endothelial dysfunction promoted by PTX3 (**Fig. 4a**). We then set out to identify the specific MMP involved, with the use of siRNA to selectively silence expression of MMP-1 and MMP-9, which are highly present MMPs in the endothelial layer. We found that silencing of MMP-9 did not alter PTX3's vascular effects (**Fig. 4b**); in contrast, silencing of MMP-1 protected from PTX3-evoked endothelial dysfunction (**Fig. 4c**). In agreement, Western blotting revealed that PTX3 enhanced MMP1 expression in WT mouse mesenteric artery (**Fig. 4d**), an effect absent in P-selectin$^{-/-}$ vessels (**Fig. 4e**), and that PTX3-induced ultrastructural alterations were absent in vessels transfected with MMP-1 siRNA (**Fig. 4f**). Taken together, these findings clearly demonstrate the involvement of a P-selectin/MMP-1 pathway in PTX3-induced damage to the membrane of endothelial cells.

PTX3 alters Nitric Oxide signaling

Nitric oxide (NO) is the main determinant of the vasorelaxant effects mediated by endothelium[21]. Our data showing selective impairment of the endothelial layer after exposure to PTX3 prompted us to explore its effect on nitric oxide signaling. In particular, we found that PTX3 blunted phosphorylation of endothelial NO synthase (eNOS) at serine 1177, an activation site of the enzyme (**Fig. 5a**), and uncoupled eNOS, as evidenced by the increase of the monomeric form (**Fig. 5b**).

At the function level, L-NAME-induced eNOS inhibition significantly blunted the acetylcholine response in control vessels, indicating the presence of NO in acetylcholine's vasorelaxant action (**Fig. S4a** *upper*). In agreement with what we observed at the molecular level, this effect was absent in PTX3-treated vessels, clearly indicating an impairment of NO signaling (**Fig. 5d** upper).

P-selectin KO mice were protected from PTX3's effect on nitric oxide signaling (**Fig. 5c**).

A comparable effect on eNOS phosphorylation was observed using SAP, which has been reported to act via the P-Selectin receptor[19] (additional data in the Results section of the online-only Data Supplement and **Figure S5**).

Nitric oxide plays a crucial role in the modulation of vascular tone, counteracting smooth muscle vasoconstriction[22]. Accordingly, we observed that the inhibition of eNOS obtained with L-NAME enhanced smooth muscle phenylephrine-evoked vasoconstriction in control vessels (**Fig. S4b** *bottom*). To be noted, this effect was impaired in PTX3-treated vessels, which show *per se* an enhanced adrenergic vascular response compared to control vessels (**Fig. 5d** bottom). These data clearly demonstrate that the greater smooth muscle contraction observed in PTX-treated vessels is dependent upon an impairment of nitric oxide signaling.

Finally, recruitment of macrophages, which may play a role in vasoconstriction[23], was not detected in vessel walls after PTX3 administration (additional data in the Results section of the Online Data Supplement and **Figure S6**).

PTX3 evokes the detachment of Caveolin-1 from plasma membrane

We performed further analysis aimed at understanding how the morphological changes correlated with impairment of endothelial signaling. Ultrastructural analyses revealed that

endothelial cells from mesenteric arteries of WT mice treated with vehicle or from mice treated with siRNA targeting MMP-1 had a well-preserved architecture and vesicles (caveolae) under the plasma membrane (**Fig. 5e** panel 1). These caveolae presented as uncoated vesicles organized in clusters forming a complicated network just below the plasma membrane (**Fig. 5e** panel 1 and panel 3). Moreover, these vesicles were delimited by a membrane that was continuous with the plasma membrane (**Fig. 5e** panel 3). The ultrastructural features of the caveolae were in line with what was observed by Rajamannan and coworkers in their detailed transmission electron microscopy study on endothelial cell[24] After exposure to PTX3, endothelial cells presented with disruption of the plasma membrane, and Cav-1 immunogold particles were found relocated to poorly preserved vesicles within intracellular cytoplasmic regions (**Fig. 5e** panel 2).

When mesenteric artery endothelial cells from control and siRNA-MMP-1-treated WT mice were processed for MMP-1 immunocytochemistry, the gold particles were found located in vesicles under the plasma membrane (**Fig. 5e** panel 4) and in vesicles continuous with the plasma membrane (**Fig. 5e** panel 6). After exposure to PTX3, endothelial cells had a great number of MMP-1 gold particles located inside the cells (**Fig. 5e** panel 5 upper); moreover, particles were located on the plasma membrane and on vesicles under it (**Fig. 5e** panel 5 bottom).

Finally, immunoprecipitation studies revealed that eNOS remained linked to Cav-1 in PTX3-treated vessels (**Fig. 5f**). The silencing of MMP1 via siRNA protected from plasma membrane disruption and rescued eNOS detachment from Cav-1 (**Fig. 5f**).

In vivo effects of PTX3 on vascular function and blood pressure.

Endothelial dysfunction is a typical marker of arterial hypertension[8]. Our in vitro findings therefore prompted us to explore the effects of PTX3 on blood pressure and vascular function in vivo. To this end, we injected mice with PTX3 or vehicle and evaluated blood pressure in a time

period previously reported to be sufficient for effects to appear in vivo[18]. We found that administration of the protein significantly increased the blood pressure of WT mice (**Fig. 6a, S7a**), an effect counteracted by the absence of P-selectin (**Fig. 6b, S7b**). In addition, when we excised vessels for vascular reactivity studies and ultrastructural analysis, we observed endothelial dysfunction (**Fig. 6c**) and morphological changes (**Fig. 6d** panel 2) similar to those encountered in the ex vivo experiments. As expected, administration of PTX3 did not evoke vascular effects in P-selectin knockout mice (**Fig. 6c** and **Fig. 6d** panel 4).

No significant differences were observed between mice with a genetic ablation of PTX3 and their controls (**Fig. S7c**), suggesting that the absence of PTX3 does not influence blood pressure levels under basal conditions.

PTX3 impairs Nitric Oxide production in HUVEC

Data obtained in vessels demonstrated that the endothelium is the target of PTX3's vascular action. Thus, we focalized our attention on HUVEC: we found that PTX3 impaired nitric oxide production in HUVEC through an involvement of the MMP-1 signaling pathway (additional data in the Results section of the Online Data Supplement and **Figures S8,S9**).

Hypertensive patients have elevated plasma levels of PTX3, P-selectin and MMP-1

The findings from our experimental models indicated that P-selectin and MMP-1 mediated PTX3's vascular effects, including the increase in blood pressure. To corroborate this finding also in humans, we measured the plasma levels of PTX3, P-selectin and MMP-1 in 31 hypertensive patients taking antihypertensive medication but that did not have good blood-pressure control, as well as in a group of subjects that were not on antihypertensive medication and had normal systolic and diastolic blood pressures (**Table 1**). We found that hypertensive patients had significantly higher plasma concentrations of PTX3, P-selectin and MMP1

compared to normotensive subjects. (**Fig. 7a** and **Table 1**). In particular, PTX3 value reaching the highest accuracy as shown by the Area Under the Receiver Operating Characteristic curve (AUROC) compared to other variables (**Fig. 7b**) (additional data in the Results section of the Online Data Supplement and **Tables S1 and S2**).

Discussion

We report here for the first time the direct role of PTX3 on vascular endothelial function, identifying the molecular mechanisms involved. In particular, we demonstrate that PTX3 induces endothelial dysfunction in resistance vessels, a district involved in the modulation of blood pressure level, and we show that the protein localizes to the endothelial monolayer, suggesting a possible interaction with a receptor.

So far, the presence of a PTX3 receptor has been reported for inflammatory cells, where PTX3 interacts either with the Fcγ receptor to amplify innate resistance against pathogens[18] or with P-selectin in a negative feedback loop to prevent excessive recruitment of neutrophils[19]. Here, we demonstrate that P-selectin is the cognate PTX3 receptor on vascular cells, since vessels from P-selectin-knockout mice were refractive to PTX3-evoked endothelial dysfunction, whereas those from FCγR knockout mice were not. It is important to emphasize that P-selectin is both a receptor and an adhesion molecule stored within the α-granules of platelets and the Weibel–Palade bodies of endothelial cells, in which it is located on membranes at a low concentration also in the basal condition[25, 26]. We also demonstrate that PTX3 induces an increase in P-selectin on the membrane of isolated endothelial cells.

An interesting observation emerging from our study is that endothelial dysfunction is still present after the removal of PTX3. This led us to hypothesize a mechanism that induced changes

in vascular structure. In fact, ultrastructural analysis of the endothelial layer of vessels revealed extensive vacuolization of the cytoplasm and disruption of basal membranes after exposure to PTX3. These findings are in agreement with a previous study showing the ability of the PTX family to induce membrane disruption in Gram-negative bacteria[27]. The morphological alterations seen in the endothelial cells were completely absent at the muscular level, pointing to the endothelium as the specific target of PTX3. Absence of P-selectin protected from PTX3-mediated morphological changes and vascular dysfunction, leading us to hypothesize that the structural alterations contributed to endothelial dysfunction.

The main mechanism related to endothelial dysfunction in hypertension is represented by alteration of the nitric oxide pathway[28, 29]. On this point, our studies revealed that PTX3 induced, *per se*, an impairment in NO signaling that evoked endothelial dysfunction and enhanced smooth muscle vasoconstriction, two typical traits involved in increased vascular resistance in hypertension[22].

We also aimed to understand how the morphological changes observed in our study correlated with the impairment in endothelial signaling. In endothelial cells, it is known that eNOS is mostly targeted to caveolae on the plasma membrane through interaction with Cav-1[30], the major protein constituent of this membrane microdomain caveolae[31]. Binding to eNOS negatively regulates the enzyme's activity, maintaining eNOS in the monomeric state[32]. In vessels treated with PTX3, we found that, following disruption of the plasma membrane, Cav-1 relocated to intracellular cytoplasmic regions and remained linked to eNOS, as evidenced by immunoprecipitation studies. This condition was associated with the presence of eNOS in its monomeric state, clearly indicative of inactivated nitric oxide intracellular signaling.

It was previously reported that absence of PTX3 is accompanied by greatly diminished

tissue inflammation and injury and decreased lethality after reperfusion of an ischemic superior mesenteric artery in mice, demonstrating that PTX3 is relevant to tissue damage[33, 34]. In agreement, PTX3-overexpressing mice had greater tissue damage and mortality after reperfusion of the ischemic vascular bed[35]. Our finding that PTX3 is harmful for the mesenteric district is fully in agreement with previous reports suggesting that therapeutic blockade of PTX3's action may be useful for injuries associated with severe ischemia and reperfusion syndromes in the this area[35].

We also identify signaling molecules recruited by the PTX3/P-selectin pathway to induce the vascular changes. Among the possible candidates, metalloproteinases play a prominent role. This is an expanding family of endopeptidases with the ability to degrade extracellular matrix components and digest the endothelial basal lamina[36]. In addition, MMPs are inflammatory mediators linking inflammation with angiogenesis and vascular remodeling, and are also implicated in the pathogenesis of vascular diseases, such as atherosclerosis, aortic aneurysms, plaque rupture and neointimal hyperplasia[37]. We demonstrate that non-selective inhibition of MMP with GM6001 protected from PTX3-evoked vascular damage. The major MMP isoforms expressed in the vasculature include MMP-1, MMP-2, MMP-3 and MMP-9, and among these, MMP-1 is predominantly secreted by endothelial cells[38, 39] and has been reported associated with organ damage during arterial hypertension[40]. We demonstrate for the first time that PTX3 increases MMP-1 expression in resistance vessels. The evidence showing that this effect is absent in P-selectin$^{-/-}$ vessels clearly demonstrates that MMP-1 is a downstream member of the PTX3/P-selectin pathway. To definitively demonstrate MMP-1's involvement in PTX3-mediated vascular changes, we silenced it with siRNA: in this experimental setting, PTX3 failed to promote endothelial nitric oxide dysfunction and morphological vascular alterations, including

Cav-1 relocation from the plasma membrane.

Our data clearly candidate the endothelium as the target of PTX3's vascular action. We focalized our attention on isolated HUVEC to specifically evaluate the effect of PTX3 on nitric oxide production. We demonstrate for the first time that PTX3 reduces NO production in isolated endothelial cells, and that this effect is associated with an enhanced expression and activity of MMP1. The silencing of the latter by siRNA protected from the deleterious action of PTX3 on NO.

We also characterized the effect of PTX3 in vivo, by injecting the protein intraperitoneally at a dose already reported to modulate P-selectin-mediated inflammatory response[18]. Also in this experimental setting, PTX3 induced endothelial dysfunction, vascular morphological changes and an increase in MMP-1 expression. Lack of P-selectin protected the vascular system from the harmful effects of PTX3. Of note, in vivo administration was not accompanied by reductions in neutrophil accumulation and an inflammatory status, suggesting that the effect observed did not depend on the inflammatory system[18]. It is important to emphasize that our in vivo findings are similar to those obtained in vitro, a setting that cannot be influenced by systemic inflammatory responses.

The transgenic PTX3-overexpressing mouse is an experimental model characterized by the presence of higher PTX3 levels than normal. A careful analysis of data revealed that overexpression of the protein is induced by different stimuli[33, 35]. So far, there are no available data on blood pressure in this experimental condition, and future studies will need to pursue this goal.

Endothelial dysfunction is a typical marker of several cardiovascular disorders, such as arterial hypertension. It is still debated whether endothelial dysfunction participates in

hypertension or is evoked by high blood pressure. Our in vivo experiments demonstrate that PTX3 significantly increases blood pressure in our observation period and that this hemodynamic effect was mediated by P-selectin. In vitro experiments demonstrated that PTX3 induces endothelial dysfunction in an experimental condition not influenced by high pressure levels. Thus, taken together, our results suggest that endothelial dysfunction induced by PTX3 participates in the increase in blood pressure observed after in vivo administration of the protein.

In addition to PTX3, other inflammatory factors are able to induce vascular dysfunction.

Interestingly, SAP interacts with P-selectin in immunological processes and induces endothelial dysfunction via the same receptor at the vascular level. However, P-Selectin does not represent the common target of all inflammatory factors, since CRP evokes its deleterious vascular effect through interaction with the FCgammaIIB receptor[20]. Thus, these inflammatory molecules recruit different mechanisms for their vascular effects; their characterization could help to better define their roles in the clinical setting.

Finally, we found that the plasma levels of P-Selectin and MMP1, two mediators of PTX3's vascular damaging effects, are higher in hypertensive patients. Our data is supported by previous studies reporting association of elevated plasma P-selectin with hypertension[41, 42], and with a study in which MMP-1 was associated with organ damage and progression of hypertension[40].

In conclusion, we describe for the first time the direct involvement of the acute phase protein PTX3 in cardiovascular homeostasis, with the modulation of vascular function and blood pressure in experimental models. Data obtained in humans suggest that PTX3, P-selectin and MMP-1 may represent new biomarkers for the prediction of vascular dysfunction onset in hypertensive patients. To be noted, these biomarkers are closely linked, since P-selectin and

MMP1 are down-stream molecules of the signaling pathway initiated by PTX3. Thus, the monitoring of these proteins could become part of a novel preventative strategy aimed at blunting the evolution of high blood pressure.

Study limitations

We analyzed only a short time-window of PTX3's effects on vascular function and blood pressure homeostasis. This decision was based on a previous study reporting that two hours was enough to evoke effects induced by PTX3 in vivo[19]. More studies are therefore warranted to fully characterize PTX3's action on cardiovascular homeostasis over a longer period. Nevertheless, the effects observed in this short time-frame were sufficient for us to define the molecular mechanisms involved. In addition, the hypertensive patients studied were receiving antihypertensive treatment, so we cannot exclude that results were influenced by drug therapy. Thus, further multicenter prospective studies are needed before PTX3, P-selectin and/or MMP-1 could be used routinely as screening biomarkers.

Acknowledgments: We thank Professor Alberto Mantovani and his research group (Istituto Clinico Humanitas) for their precious support and for the supply of transgenic mice and PTX3 reagents.

Funding Sources: G.M. is supported by grants from Fondazione Italiana Sclerosi Multipla (FISM) 2012/R/11, the European Union IDEAS Programme European Research Council Starting Grant "menTORingTregs" 310496, and CNR-Program "Medicina Personalizzata".

Conflict of Interest Disclosures: None.

References:

1. Moalli F, Jaillon S, Inforzato A, Sironi M, Bottazzi B, Mantovani A, Garlanda C. Pathogen recognition by the long pentraxin PTX3. *J Biomed Biotechnol*. 2011;2011:830421.

2. Inforzato A, Bottazzi B, Garlanda C, Valentino S, Mantovani A. Pentraxins in humoral innate immunity. *Adv Exp Med Biol*. 2012;946:1-20.

3. Mantovani A, Valentino S, Gentile S, Inforzato A, Bottazzi B, Garlanda C. The long pentraxin PTX3: a paradigm for humoral pattern recognition molecules. *Ann N Y Acad Sci*. 2013;1285:1-14.

4. Bottazzi B, Vouret-Craviari V, Bastone A, De Gioia L, Matteucci C, Peri G, Spreafico F, Pausa M, D'Ettorre C, Gianazza E, Tagliabue A, Salmona M, Tedesco F, Introna M, Mantovani A. Multimer formation and ligand recognition by the long pentraxin PTX3. Similarities and differences with the short pentraxins C-reactive protein and serum amyloid P component. *J Biol Chem*. 1997;272:32817-32823.

5. Introna M, Alles VV, Castellano M, Picardi G, De Gioia L, Bottazzai B, Peri G, Breviario F, Salmona M, De Gregorio L, Dragani TA, Srinivasan N, Blundell TL, Hamilton TA, Mantovani A. Cloning of mouse ptx3, a new member of the pentraxin gene family expressed at extrahepatic sites. *Blood*. 1996;87:1862-1872.

6. Garlanda C, Bottazzi B, Bastone A, Mantovani A. Pentraxins at the crossroads between innate immunity, inflammation, matrix deposition, and female fertility. *Annu Rev Immunol*. 2005;23:337-366.

7. Basile A, Sica A, d'Aniello E, Breviario F, Garrido G, Castellano M, Mantovani A, Introna M. Characterization of the promoter for the human long pentraxin PTX3. Role of NF-kappaB in tumor necrosis factor-alpha and interleukin-1beta regulation. *J Biol Chem*. 1997;272:8172-8178.

8. Norata GD, Garlanda C, Catapano AL. The long pentraxin PTX3: a modulator of the immunoinflammatory response in atherosclerosis and cardiovascular diseases. *Trends Cardiovasc Med*. 2010;20:35-40.

9. Parlak A, Aydogan U, Iyisoy A, Dikililer MA, Kut A, Cakir E, Saglam K. Elevated pentraxin-3 levels are related to blood pressure levels in hypertensive patients: an observational study. *Anadolu Kardiyol Derg*. 2012;12:298-304.

10. Presta M, Camozzi M, Salvatori G, Rusnati M. Role of the soluble pattern recognition receptor PTX3 in vascular biology. *J Cell Mol Med*. 2007;11:723-738.

11. Booth AD, Jayne DR, Kharbanda RK, McEniery CM, Mackenzie IS, Brown J, Wilkinson IB. Infliximab improves endothelial dysfunction in systemic vasculitis: a model of vascular inflammation. *Circulation*. 2004;109:1718-1723.

12. Witasp A, Ryden M, Carrero JJ, Qureshi AR, Nordfors L, Naslund E, Hammarqvist F, Arefin S, Kublickiene K, Stenvinkel P. Elevated circulating levels and tissue expression of pentraxin 3 in uremia: a reflection of endothelial dysfunction. *PLoS One*. 2013;8:e63493.

13. Hamad RR, Eriksson MJ, Berg E, Larsson A, Bremme K. Impaired endothelial function and elevated levels of pentraxin 3 in early-onset preeclampsia. *Acta Obstet Gynecol Scand*. 2012;91:50-56.

14. Cozzi V, Garlanda C, Nebuloni M, Maina V, Martinelli A, Calabrese S, Cetin I. PTX3 as a potential endothelial dysfunction biomarker for severity of preeclampsia and IUGR. *Placenta*. 2012;33:1039-1044.

15. Suliman ME, Yilmaz MI, Carrero JJ, Qureshi AR, Saglam M, Ipcioglu OM, Yenicesu M, Tong M, Heimburger O, Barany P, Alvestrand A, Lindholm B, Stenvinkel P. Novel links between the long pentraxin 3, endothelial dysfunction, and albuminuria in early and advanced chronic kidney disease. *Clin J Am Soc Nephrol*. 2008;3:976-985.

16. Iiyama K, Nagano M, Yo Y, Nagano N, Kamide K, Higaki J, Mikami H, Ogihara T. Impaired endothelial function with essential hypertension assessed by ultrasonography. *Am Heart J*. 1996;132:779-782.

17. Moalli F, Doni A, Deban L, Zelante T, Zagarella S, Bottazzi B, Romani L, Mantovani A, Garlanda C. Role of complement and Fc{gamma} receptors in the protective activity of the long pentraxin PTX3 against Aspergillus fumigatus. *Blood*. 2010;116:5170-5180.

18. Deban L, Russo RC, Sironi M, Moalli F, Scanziani M, Zambelli V, Cuccovillo I, Bastone A, Gobbi M, Valentino S, Doni A, Garlanda C, Danese S, Salvatori G, Sassano M, Evangelista V, Rossi B, Zenaro E, Constantin G, Laudanna C, Bottazzi B, Mantovani A. Regulation of leukocyte recruitment by the long pentraxin PTX3. *Nat Immunol*. 2010;11:328-334.

19. Ji Z, Ke ZJ, Geng JG. SAP suppresses the development of experimental autoimmune encephalomyelitis in C57BL/6 mice. *Immunol Cell Biol*. 2012;90:388-395.

20. Sundgren NC, Zhu W, Yuhanna IS, Chambliss KL, Ahmed M, Tanigaki K, Umetani M, Mineo C, Shaul PW. Coupling of Fcgamma receptor I to Fcgamma receptor IIb by SRC kinase mediates C-reactive protein impairment of endothelial function. *Circ Res*. 2011;109:1132-1140.

21. Ignarro LJ. Nitric oxide as a unique signaling molecule in the vascular system: a historical overview. *J Physiol Pharmacol*. 2002;53:503-514.

22. Volpe M, Iaccarino G, Vecchione C, Rizzoni D, Russo R, Rubattu S, Condorelli G, Ganten U, Ganten D, Trimarco B, Lindpaintner K. Association and cosegregation of stroke with impaired endothelium-dependent vasorelaxation in stroke prone, spontaneously hypertensive rats. *J Clin Invest*. 1996;98:256-261.

23. Zaloudikova M, Herget J, Vizek M. The contractile response of isolated small pulmonary

arteries induced by activated macrophages. *Physiol Res*. 2014;63:267-270.

24. Rajamannan NM, Springett MJ, Pederson LG, Carmichael SW. Localization of caveolin 1 in aortic valve endothelial cells using antigen retrieval. *J Histochem Cytochem*. 2002;50:617-628.

25. Zerr M, Hechler B, Freund M, Magnenat S, Lanois I, Cazenave JP, Leon C, Gachet C. Major contribution of the P2Y(1)receptor in purinergic regulation of TNFalpha-induced vascular inflammation. *Circulation*. 2011;123:2404-2413.

26. Ushiyama S, Laue TM, Moore KL, Erickson HP, McEver RP. Structural and functional characterization of monomeric soluble P-selectin and comparison with membrane P-selectin. *J Biol Chem*. 1993;268:15229-15237.

27. Harrington JM, Chou HT, Gutsmann T, Gelhaus C, Stahlberg H, Leippe M, Armstrong PB. Membrane pore formation by pentraxin proteins from Limulus, the American horseshoe crab. *Biochem J*. 2008;413:305-313.

28. Forstermann U, Munzel T. Endothelial nitric oxide synthase in vascular disease: from marvel to menace. *Circulation*. 2006;113:1708-1714.

29. Puca AA, Carrizzo A, Ferrario A, Villa F, Vecchione C. Endothelial nitric oxide synthase, vascular integrity and human exceptional longevity. *Immun Ageing*. 2012;9:26.

30. Feron O, Belhassen L, Kobzik L, Smith TW, Kelly RA, Michel T. Endothelial nitric oxide synthase targeting to caveolae. Specific interactions with caveolin isoforms in cardiac myocytes and endothelial cells. *J Biol Chem*. 1996;271:22810-22814.

31. Minshall RD, Sessa WC, Stan RV, Anderson RG, Malik AB. Caveolin regulation of endothelial function. *Am J Physiol Lung Cell Mol Physiol*. 2003;285:L1179-83.

32. Komers R, Schutzer WE, Reed JF, Lindsley JN, Oyama TT, Buck DC, Mader SL, Anderson S. Altered endothelial nitric oxide synthase targeting and conformation and caveolin-1 expression in the diabetic kidney. *Diabetes*. 2006;55:1651-1659.

33. Souza DG, Amaral FA, Fagundes CT, Coelho FM, Arantes RM, Sousa LP, Matzuk MM, Garlanda C, Mantovani A, Dias AA, Teixeira MM. The long pentraxin PTX3 is crucial for tissue inflammation after intestinal ischemia and reperfusion in mice. *Am J Pathol*. 2009;174:1309-1318.

34. Zhu H, Cui D, Liu K, Wang L, Huang L, Li J. Long pentraxin PTX3 attenuates ischemia reperfusion injury in a cardiac transplantation model. *Transpl Int*. 2014;27:87-95.

35. Souza DG, Soares AC, Pinho V, Torloni H, Reis LF, Teixeira MM, Dias AA. Increased mortality and inflammation in tumor necrosis factor-stimulated gene-14 transgenic mice after ischemia and reperfusion injury. *Am J Pathol*. 2002;160:1755-1765.

36. Pardo A, Selman M. MMP-1: the elder of the family. *Int J Biochem Cell Biol*. 2005;37:283-288.

37. Galis ZS, Khatri JJ. Matrix metalloproteinases in vascular remodeling and atherogenesis: the good, the bad, and the ugly. *Circ Res*. 2002;90:251-262.

38. Lee SW, Song KE, Shin DS, Ahn SM, Ha ES, Kim DJ, Nam MS, Lee KW. Alterations in peripheral blood levels of TIMP-1, MMP-2, and MMP-9 in patients with type-2 diabetes. *Diabetes Res Clin Pract*. 2005;69:175-179.

39. Death AK, Fisher EJ, McGrath KC, Yue DK. High glucose alters matrix metalloproteinase expression in two key vascular cells: potential impact on atherosclerosis in diabetes. *Atherosclerosis*. 2003;168:263-269.

40. Morillas P, Quiles J, de Andrade H, Castillo J, Tarazon E, Rosello E, Portoles M, Rivera M, Bertomeu-Martinez V. Circulating biomarkers of collagen metabolism in arterial hypertension: relevance of target organ damage. *J Hypertens*. 2013;31:1611-1617.

41. Blann AD, Nadar SK, Lip GY. The adhesion molecule P-selectin and cardiovascular disease. *Eur Heart J*. 2003;24:2166-2179.

42. Ridker PM, Buring JE, Rifai N. Soluble P-selectin and the risk of future cardiovascular events. *Circulation*. 2001;103:491-495.

Table 1. Characteristics of hypertensive patients and matched control subjects.

Parameter	Hypertensives	Controls	*p*
Age, years	58.63±12.8	55.81±14.6	NS
Sex, M/F	22/9	15/6	NS
Smokers, M/F	10/4	8/3	NS
Anti-hypertensive medication, n	31	0	
Systolic BP, mmHg	147.5±24	116±11	0.0064
Diastolic BP, mmHg	86.8±11	72±8	0.0062
Plasma PTX3, ng/mL	3.97±2.3	1.72±0.66	<0.0001
Plasma P-selectin, ng/mL	64.5±15.6	52.06±10	0.0119
Plasma MMP-1, pg/mL	304.1±134	116.7±63	0.0002

Data are reported as mean±SD. M, male; F, female; BP, blood pressure; NS, not statistically significant.

DOI: 10.1161/CIRCULATIONAHA.114.014822

Figure Legends

Figure 1. a–c) Dose–response curves to acetylcholine (Ach) of phenylephrine-precontracted mesenteric arteries from C57BL/6N mice. Vessels were pre-exposed to pentraxin 3 (PTX3) for 15, 30, 45 or 60 minutes at different dosages (2, 20 or 200 ng/mL). **, *p*<0.01, ***, *p*<0.001 vs vehicle, 15', 30'; n=7 for each group). **d)** Immunohistochemical staining, using fluorescent streptavidin, of mesenteric arteries from C57BL/6N mice treated with vehicle or with biotinylated PTX3. Scale bar□100μm.

Figure 2. a) Dose–response curves to acetylcholine (Ach) of phenylephrine-precontracted Fcγ$^{+/+}$ and Fcγ$^{-/-}$ mesenteric arteries exposed to vehicle or pentraxin 3 (PTX3) for 45 minutes; *, p<0.05; **, p<0.01 vs FCγ$^{-/-}$+ vehicle and FCγ$^{+/+}$+ vehicle; n=5 for each group. **b)** Dose–response curves to Ach of phenylephrine-precontracted P-selectin$^{+/+}$ and P-selectin$^{-/-}$ mesenteric arteries after 45 minutes of exposure to vehicle or PTX3. *, p<0.05; **, p<0.01 vs P-sel$^{-/-}$ + vehicle, P-sel$^{-/-}$ + PTX3 and P-sel$^{+/+}$ + vehicle; n=5 for each group. **c)** Endogenous P-selectin immunoprecipited with PTX3 in mesenteric artery lysate from wild-type (WT) but not from P-selectin knockout (KO) mice. Extracts were immunoprecipitated for P-selectin and then probed with anti-P-selectin or anti-PTX3 antibodies; n=3.

Figure 3. a) Dose–response curves to acetylcholine (Ach) of phenylephrine-precontracted mesenteric arteries from C57BL/6N mice (WT); vessels were either untreated, exposed to pentraxin 3 (PTX3) for 45 minutes (WT+PTX3), or exposed to PTX3 with continuous wash-out (WT+PTX3 wash-out). **, *p*<0.01 vs WT. ##, p<0.01 vs WT; n=6 for each group. **b)** Effect of

PTX3 on the ultrastructure of endothelial cells. Representative micrographs of endothelial cells from WT and P-selectin knockout (KO) mice under basal conditions (panels 1 and 3) or after exposure to PTX3 (panels 2 and 4). WT and P-selectin KO endothelial cells under basal conditions and P-selectin KO endothelial cells exposed to PTX3 had well-preserved cytoplasm and nuclei; WT mesenteric artery endothelial cells exposed to PTX3 had a dilution of the cytoplasm and disruption of the plasma membrane (arrows); n=4 for each group. C=cytoplasm, N=nucleus, V=vacuole. Scale bars, =1.17(1) and =0.76 μm(2).

Figure 4. a) Dose–response curves to acetylcholine (Ach) of phenylephrine-precontracted mesenteric arteries from C57BL/6N mice: vessels were exposed to vehicle only, to PTX3 for 45 minutes (PTX3), to GM6001 plus PTX3 (GM6001+PTX3), or to GM6001 alone (n=6 for each group). *, $p<0.05$ vs vehicle, GM6001+ PTX3, GM6001; **, $p<0.01$ vs vehicle, GM6001+PTX3, GM6001. **b, c)** Dose–response curves to Ach of phenylephrine-precontracted mesenteric arteries from C57BL/6Nmice: vessels were exposed to vehicle or transfected with siRNA against MMP-9 (**, $p<0.01$ vs Vehicle, scr. siRNA; ##, p<0.01 vs Vehicle, scr. siRNA) or MMP-1 and then exposed to PTX3; scrambled siRNA was used as a control. **, $p<0.01$ vs Vehicle, scr. siRNA and siRNA MMP-1 + PTX3; n=8 for each group. **d)** Representative Western blots for MMP-1 in wild-type (WT) mesenteric arteries exposed to vehicle, PTX3, siRNA to silence MMP-1 and/or to a scrambled siRNA (n=3). *, $p<0.05$; **, $p<0.01$. **e)** Representative Western blots for MMP-1 in mesenteric arteries from WT and P-selectin$^{-/-}$ vessels exposed to vehicle or PTX3 (n=3). **, $p<0.01$. **f)** Effect of silencing MMP-1 on the ultrastructural alterations induced by PTX3: panel 1) control endothelial cells had well-preserved cytoplasm and nucleus; panel 2) cells exposed to PTX3 had diluted cytoplasm with numerous vacuoles

(arrows) and broken membranes (thick arrow); panel 3) silencing of MMP-1 with an siRNA inhibited PTX3-induced changes. C= cytoplasm, N= Nucleus. Scale bar= 1.1 µm (n=4 for each group).

Figure 5. a-b) Representative Western blots for p-eNOS and eNOS monomer/dimer in wild-type (WT) mesenteric arteries exposed to vehicle, to PTX3 or to siRNA plus PTX3. *Bottom*: densitometric analyses of 3 independent experiments. *, $p<0.05$ (n=4). **c)** Representative Western blots for p-eNOS on serine 1177 (*left*) or eNOS monomer/dimer (*right*) in mesenteric arteries from WT and P-selectin KO mice treated with vehicle or treated with PTX3. *Bottom:* Densitometric analyses of 3 independent experiments. *, $p<0.05$. (n=3). **d)** Dose–response curves to acetylcholine (Ach) (*upper*) or to phenylephrine (*bottom*) in control condition (alone), or in presence of PTX3 or PTX3 plus L-NAME (300 µM). **, $p<0.01$, vs WT; n=5 for each group. **e)** ***Panel 1*)** Endothelial cells from WT mesenteric artery had anti-CAV-1 immunogold particles (arrows) located in short spherical vesicles (caveolae) under the plasma membrane; ***Panel 2)*** After exposure to PTX3, endothelial cells had a disrupted plasma membrane (asterisk), and anti-CAV-1 immunogold particles (thick arrows) distributed under the plasma membrane in poorly preserved vesicles; ***Panel 3*)** Endothelial cell of a WT siRNA MMP-1 mesenteric artery with anti-CAV-1 immunogold particles staining a vesicle under the plasma membrane. Arrowheads point to the membrane delimiting the vesicles. The thin arrow points to an immunogold particle located outside the endothelial membrane, in the vessel lumen. Scale bar (A)= 0.182 µm, (B)= 0.17 µm, (C)= 0.167 µm. ***Panel 4)*** Mesenteric artery endothelial cell from WT mouse with a cluster of anti-MMP-1 immunogold particles located in vesicles under the plasma membrane (arrows); ***Panel 5)*** *upper:* after exposure to PTX3, endothelial cells had a

greater number of anti-MMP-1 gold particles located inside the cells, on the plasma membrane and on vesicles under the plasma membrane (*bottom*) (arrows); ***Panel 6)*** endothelial cell from siRNA MMP-1 mice showing MMP-1 immunogold particles located in vesicles continuous with the plasma membrane (arrows); n=3 for each experimental condition. **f)** Endogenous eNOS immunoprecipitated with CAV-1 in mesenteric artery lysate from C57BL/6N: vessels were exposed to vehicle alone, to PTX3 alone or were transfected with siRNA MMP-1 and exposed to PTX3. Extracts were immunoprecipitated for CAV-1 and then probed with anti-eNOS or anti-CAV-1 antibodies; n=3.

Figure 6. Mean arterial pressure (MAP) of wild-type mice (**a**) and P-selectin KO mice (**b**) treated with vehicle or with PTX3. *, $p<0.05$ vs WT plus vehicle; n=5 for each treatment. **c)** Dose–response curves to acetylcholine (Ach) of phenylephrine-precontracted mesenteric arteries from WT and P-selectin$^{-/-}$ mice after in vivo injection of PTX3. **, $p<0.01$ vs WT + vehicle, P-selectin$^{-/-}$ + vehicle and P-selectin$^{-/-}$ + PTX3; n=5 for each group. **d)** In vivo effect of PTX3 administration on the ultrastructure of endothelial cells: ***panels 1 and 3*)** representative micrographs of endothelial cells from WT and P-selectin$^{-/-}$ mice under basal conditions; ***panels 2 and 4*)** after PTX3 administration. In panel B, note a large cytoplasmic vacuole (V) and the broken plasma membrane (arrow) of an endothelial cell from a PTX3-treated WT mouse; no subcellular alterations are encountered in endothelial cells from mice belong to the other experimental groups. C= cytoplasm, N= nucleus, V= vacuole. Scale bar=0.45 μm; n=4 for each group.

Figure 7. a) Boxplots representing PTX3 (left), P-selectin (middle) and MMP-1 (right)

DOI: 10.1161/CIRCULATIONAHA.114.014822

distributions in hypertensive and control subjects. Each boxplot gives for each distribution, from bottom to top, the values corresponding to: lower non-outlier bound, 25th percentile, median, 75th percentile and upper non-outliers bound. Dots represent single outlier measures. **b)** Receiver Operating Characteristic curves corresponding to PTX3 (in red), SEL-P (in green) and MMP-1 (in blue). The legend gives the AUROC values and 95% Confidence Interval (95% CI) of the three analyzed variables.

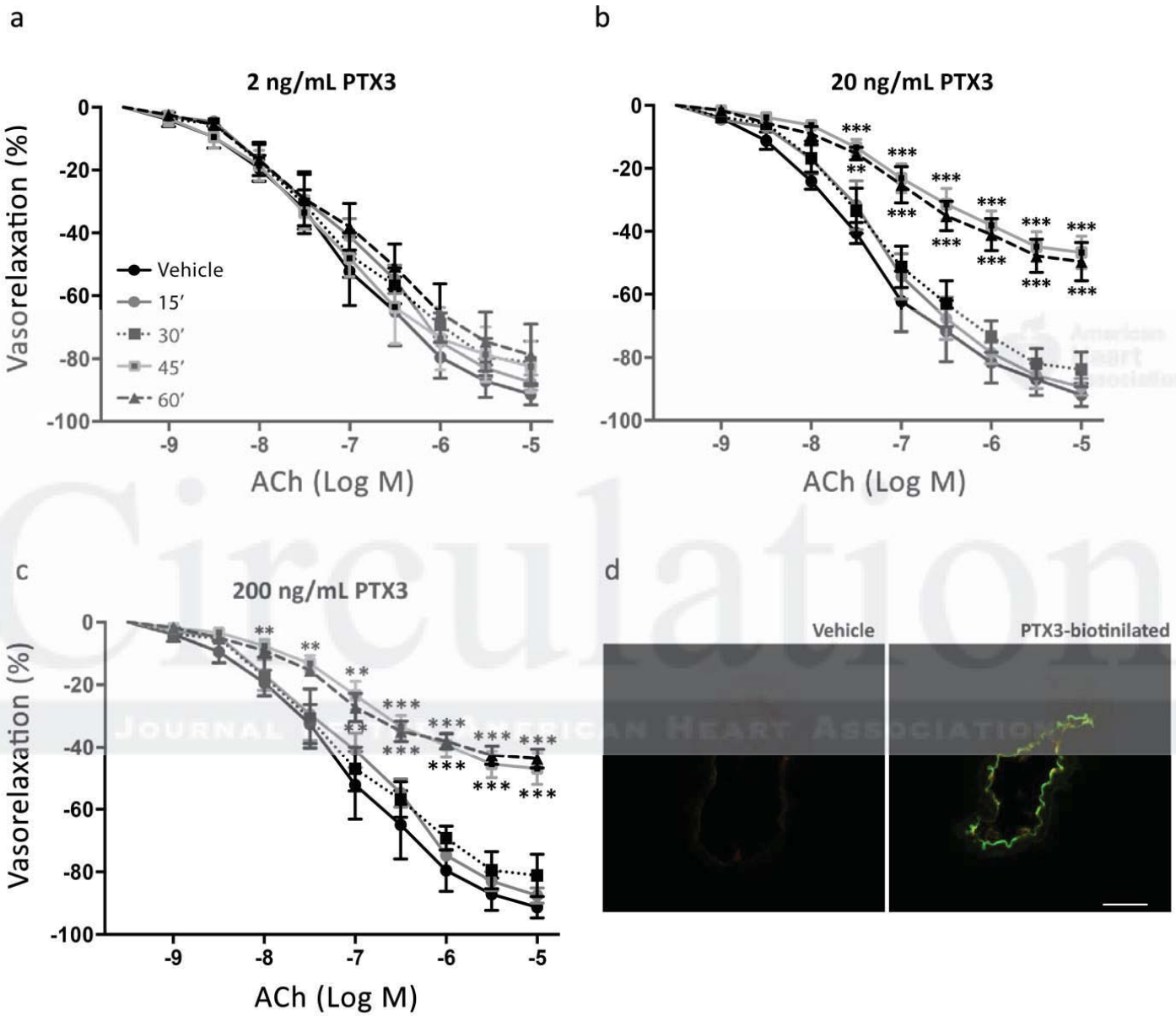

Figure 1

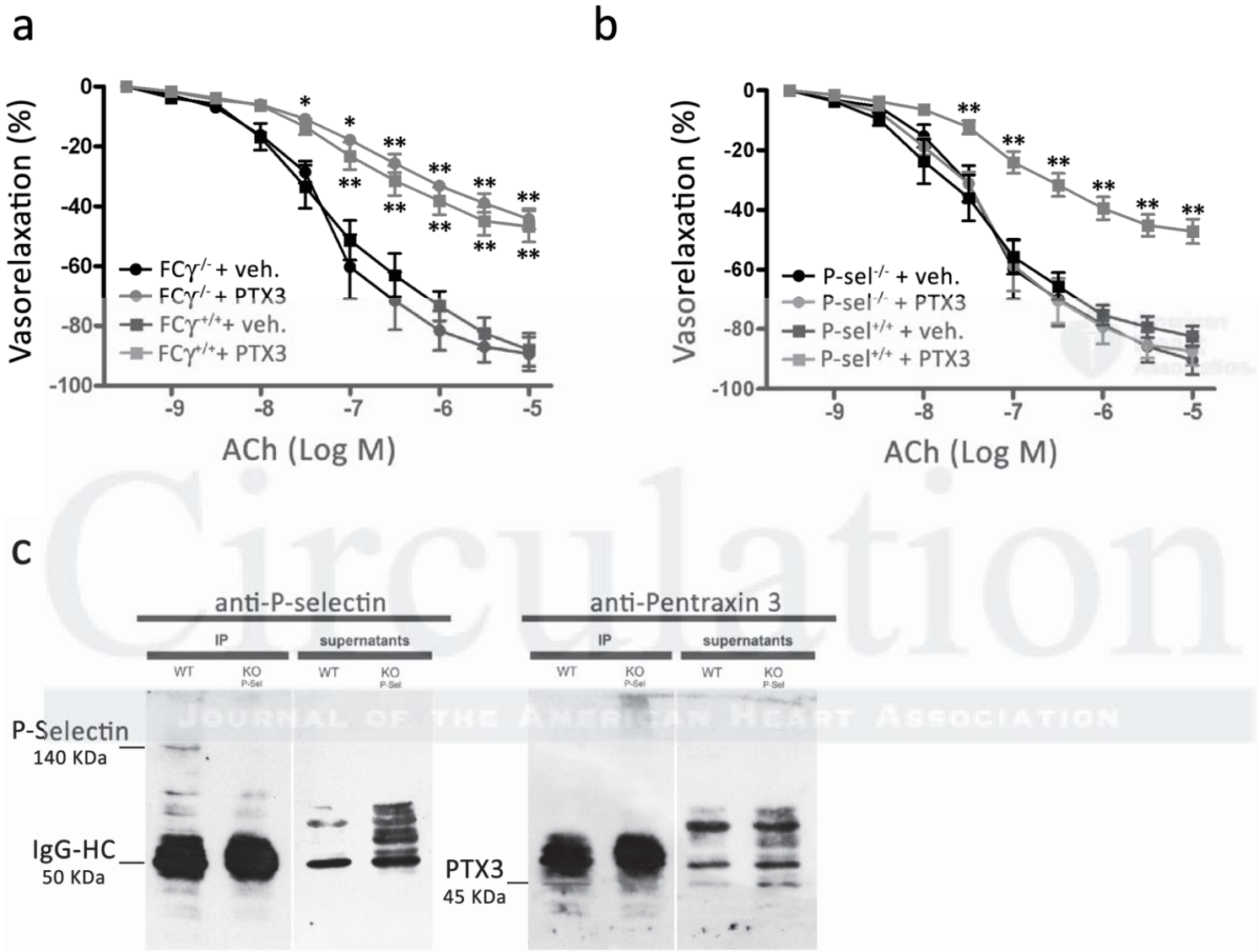

Figure 2

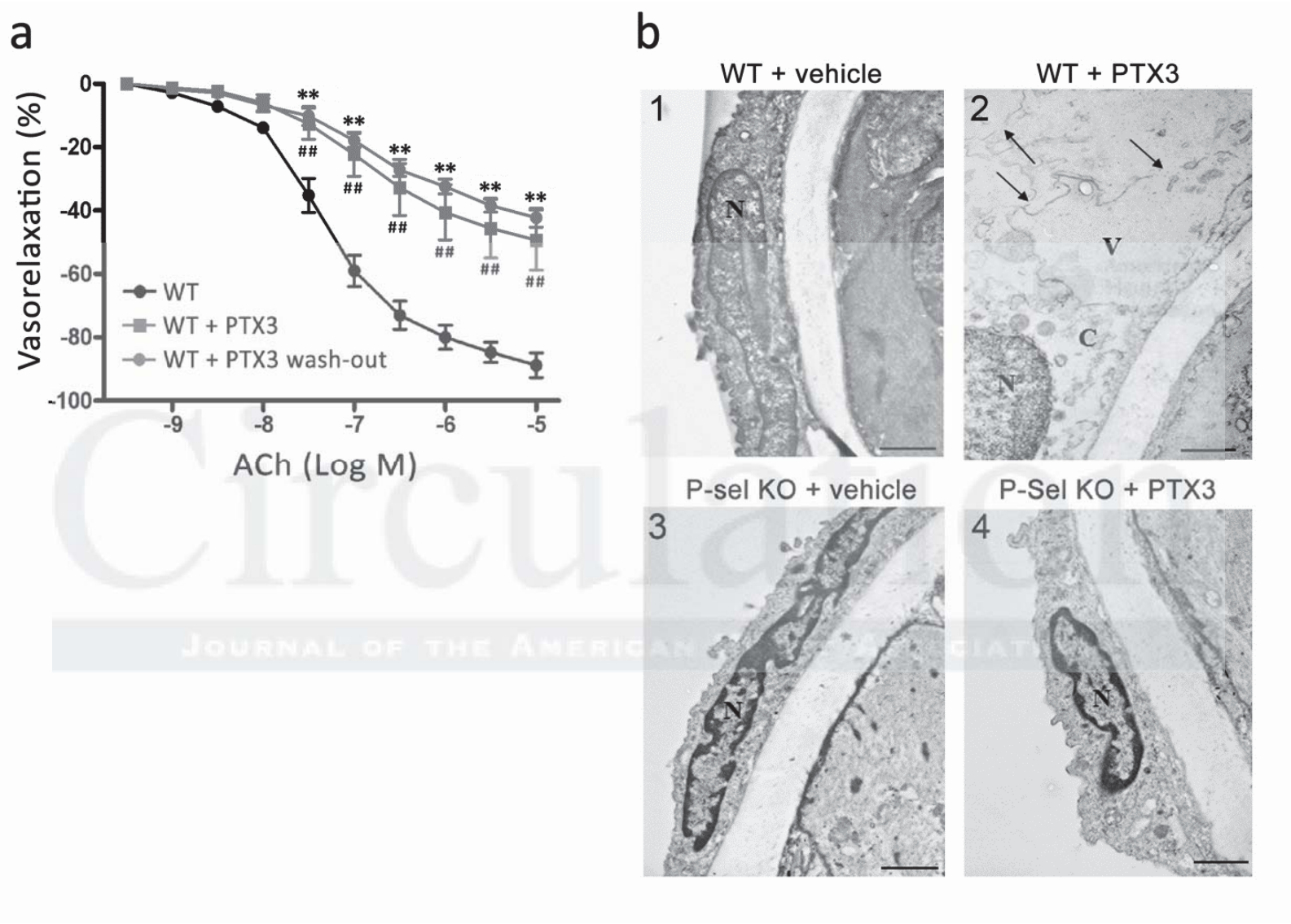

Figure 3

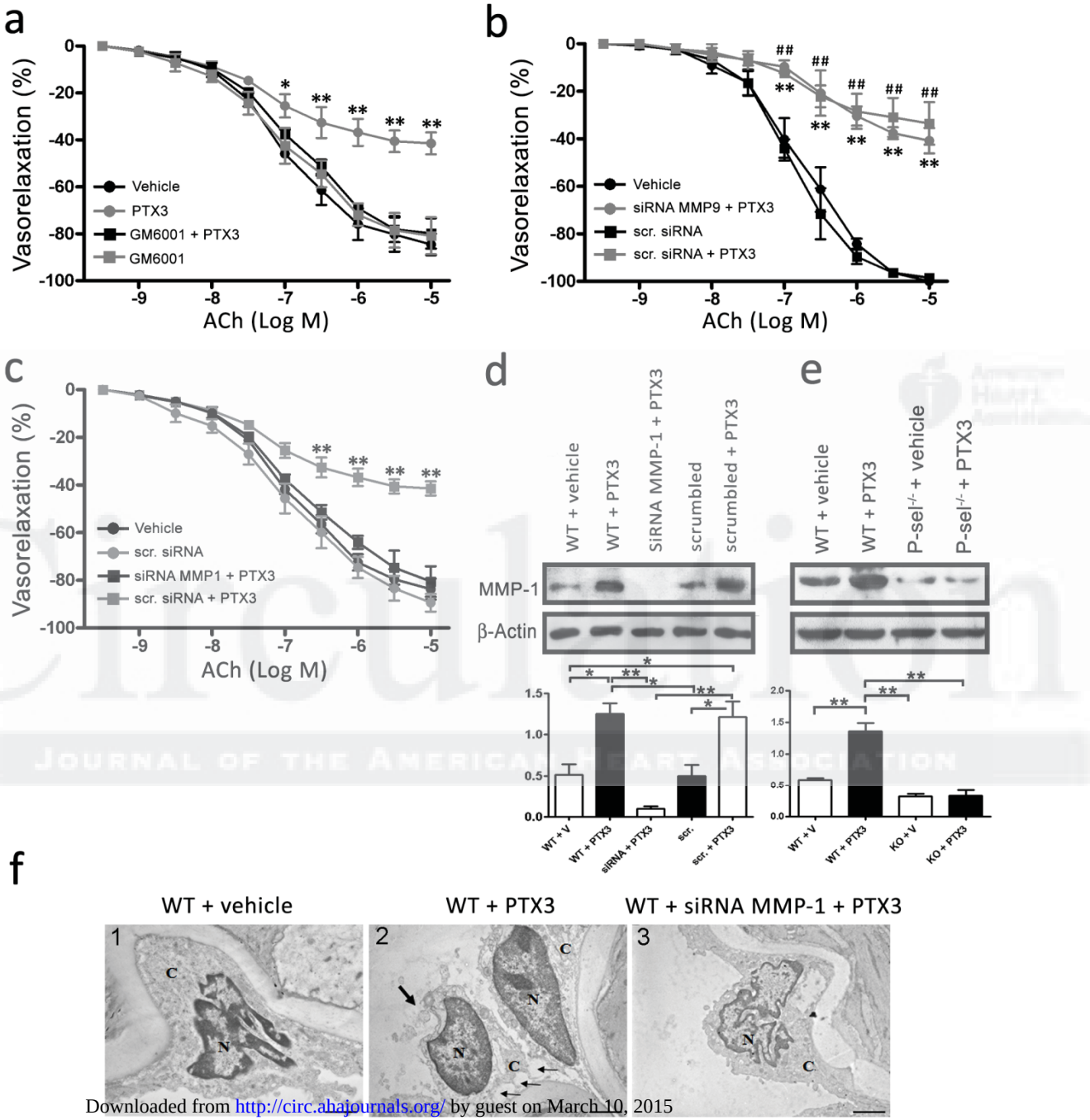

Figure 4

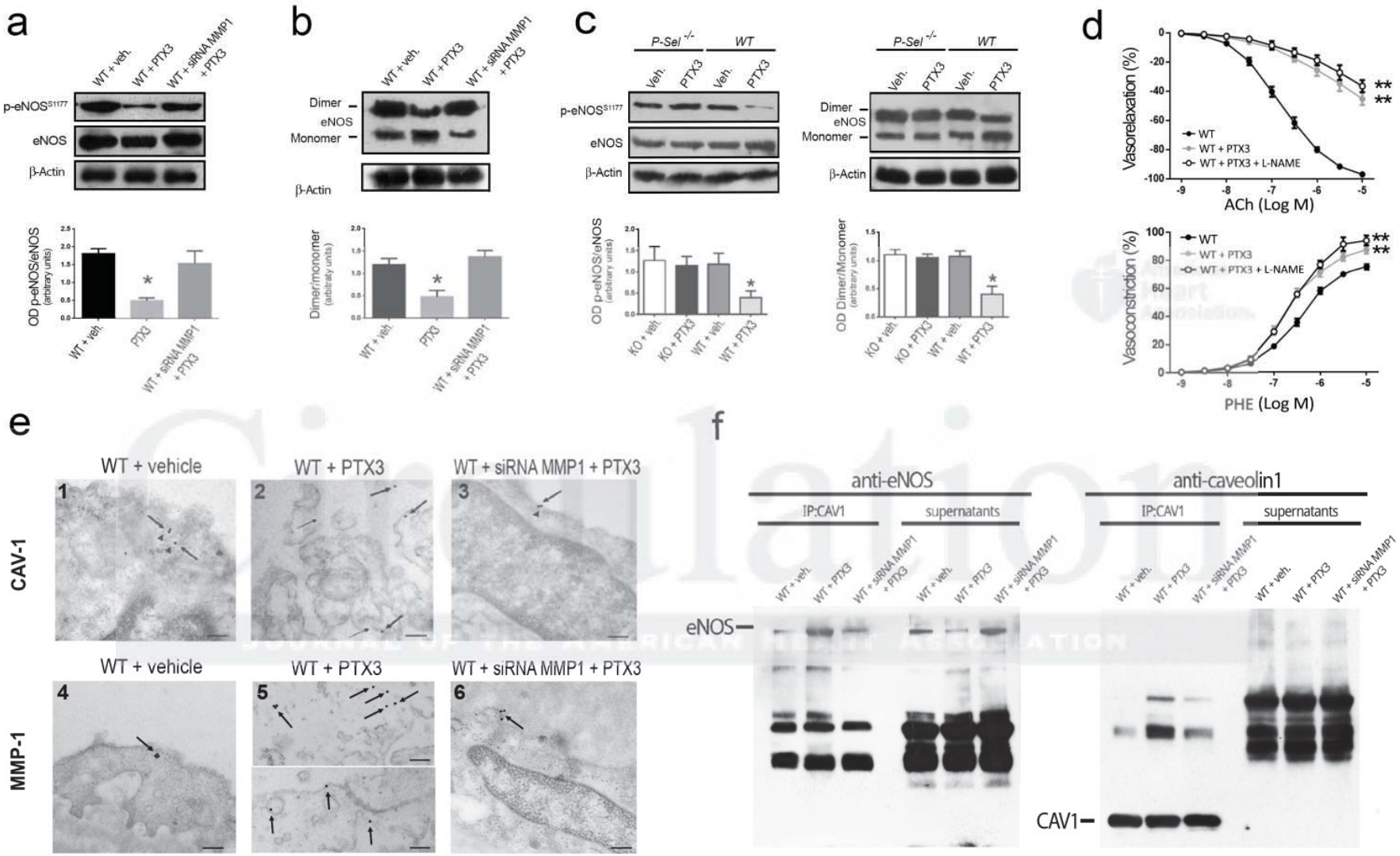

Figure 5

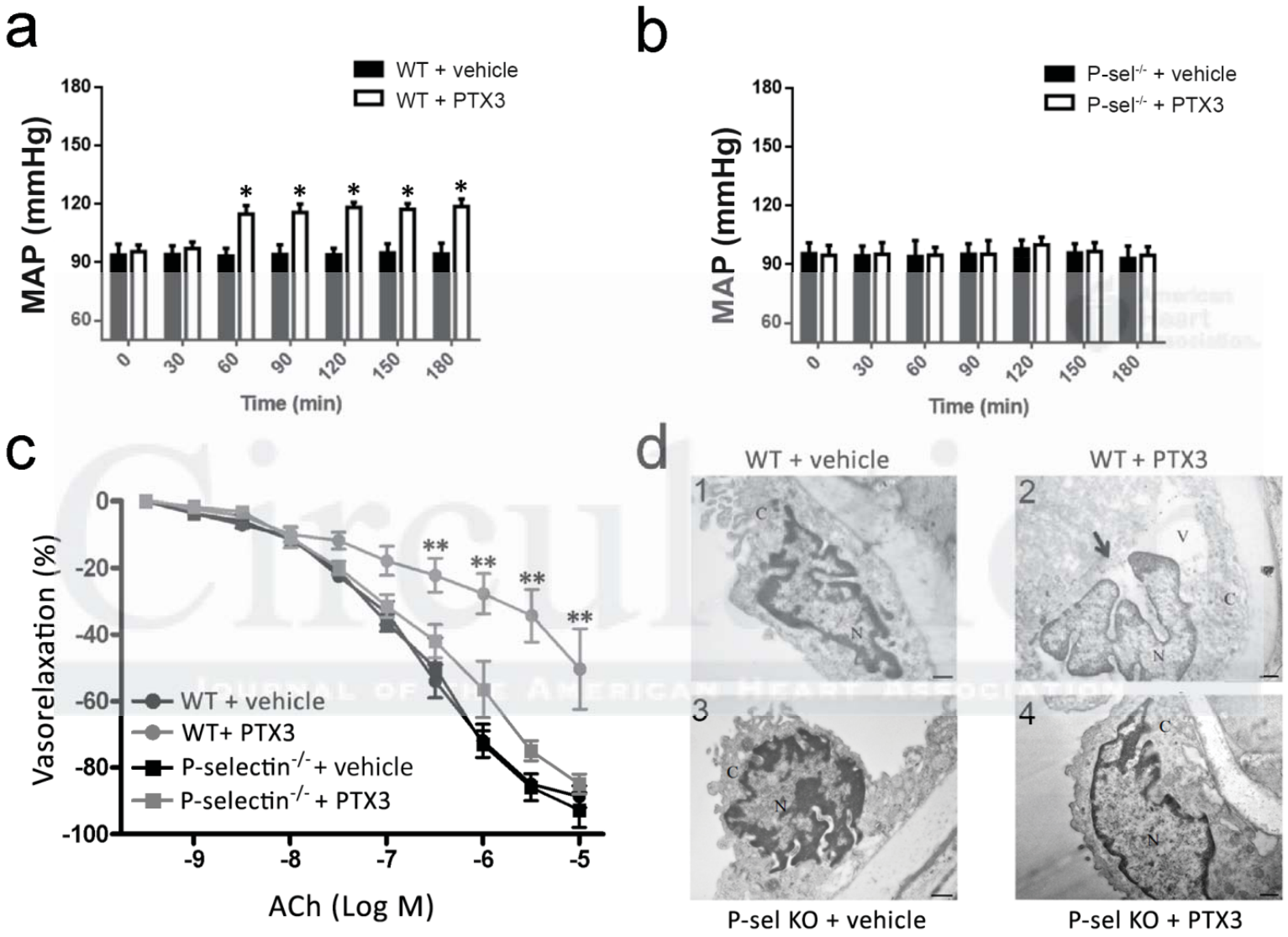

Figure 6

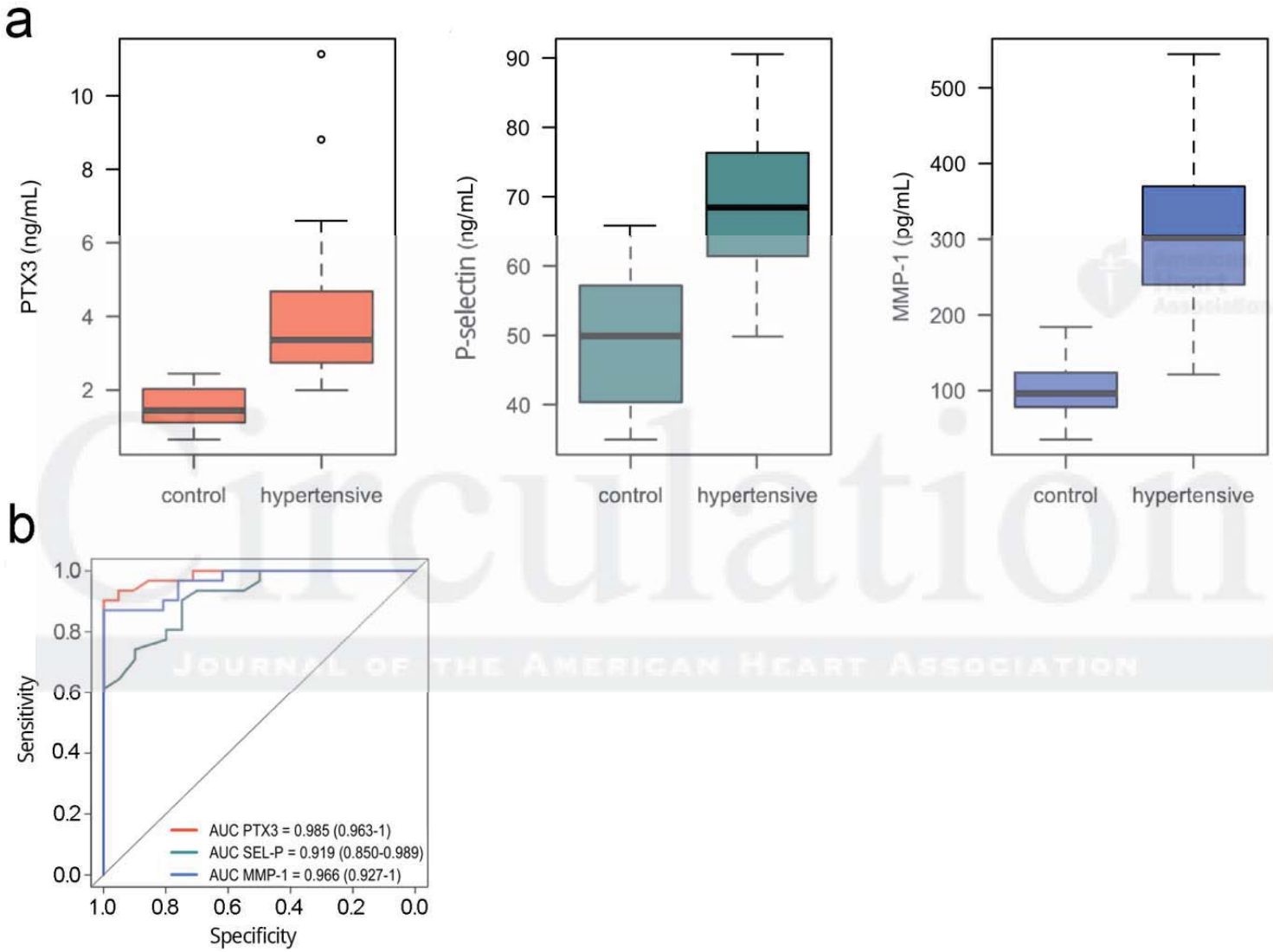

Figure 7

Pentraxin 3 induces vascular endothelial dysfunction through a P-selectin/MMP-1 pathway

Albino Carrizzo[1], M.Sc, Paola Lenzi[2], Ph.D, Claudio Procaccini[3], Ph.D, Antonio Damato[1], B.Sc, Francesca Biagioni[1], Ph.D, Ambrosio Mariateresa[1], B.Sc, Giusy Amodio[4,5], Ph.D, Paolo Remondelli[5], Ph.D, Carmine Del Giudice[6], M.Sc, Raffaele Izzo[6], M.D, Alberto Malovini[7], Ph.D, Luigi Formisano[8], Ph.D, Vincenzo Gigantino[3,9], M.Sc, Michele Madonna[1], DVM, Ph.D, Annibale A. Puca[5,10], M.D, Bruno Trimarco[6], M.D, Giuseppe Matarese[5,10], M.D, Francesco Fornai[1,2], Ph.D, M.D, Carmine Vecchione[1,5], M.D.

[1] IRCCS Neuromed, Pozzilli (IS), Italy

[2] University of Pisa, Department of Human Morphology and Applied Biology, Pisa, Italy

[3] Laboratorio di Immunologia, Istituto di Endocrinologia e Oncologia Sperimentale, (IEOS-CNR), Consiglio Nazionale delle Ricerche c/o Dipartimento di Medicina Molecolare e Biotecnologie Mediche, Università di Napoli "Federico II", Napoli, Italy

[4]Università degli Studi di Salerno, Department of Pharmaceutical Sciences, Fisciano (Salerno), Italy

[5]Università degli Studi di Salerno, Medicine and Surgery, Baronissi (Salerno), Italy

[6] Department of Clinical Medicine, Cardiovascular and Immunological Sciences, "Federico II" University of Naples, Italy

[7] University of Pavia, Department of Industrial and Information Engineering, Pavia, Italy

[8] Department of Science and Technology, University of Sannio, Benevento, Italy

[9] Pathology Unit, "Istituto Nazionale Tumori, IRCCS, Fondazione Pascale", Naples, Italy.

[10] IRCCS Multimedica, Milan, Italy

Corresponding author:

Prof. Carmine Vecchione, MD

cvecchione@unisa.it

Vascular Physiopatology unit, IRCCS Neuromed, 86077 Pozzilli (IS), Italy

Università degli Studi di Salerno, Dipartimento di Medicina, Via S. Allende, 84081 Baronissi (SA), Italy.

SUPPLEMENTAL MATERIAL

Supplemental Material and Methods

Proteins and reagents. Recombinant human PTX3 and biotinylated PTX3 were obtained as previously described [1]. Recombinant Serum amyloid protein (SAP) and C-reactive protein (CRP) were obtained from Sigma**.** MMP-1 and MMP-9 siRNA was obtained from Santa Cruz Biotechnology, Inc. Control (non-silencing) siRNA was purchased from QIAGEN. Sepharose A was purchased from Sigma. Horseradish peroxidase (HRP)-labeled anti-rabbit fragment immunoglobulin, HRP linked streptavidin, and enhanced chemiluminescence for Western blotting detection reagent were purchased from Amersham Biosciences. OPTI-MEM, Lipofectamine LTX reagent, and FBS were purchased from Invitrogen.

Animals. Fcγ-R- and P-selectin-deficient mice were obtained from Instituto Humanitas. Procedures involving animals and their care conformed to institutional guidelines. All effort was made to minimize the number of animals used and their suffering.

Vascular reactivity study. Second-order branches of the mesenteric arterial tree were removed from C57BL6 mice and from FCγR- and P-selectin-knock-out mice for vascular studies performed as described previously [2]. Briefly, vessels were placed in a wire or pressure myograph system filled with Krebs solution maintained at pH 7.4 at 37°C. Adventitial fat was carefully removed and arteries were cut into rings (~2-mm thickness). The rings were suspended by two tungsten wires (25-μm in diameter) and mounted with 0.3 g of resting tension in a wire myograph system (5-mL

chamber size; DMT Danish Myosystem). Isometric tension was measured using a force transducer coupled to a data acquisition system. After an equilibration period of 60 minutes, rings were pre-contracted with phenylephrine (1×10^{-9} to 10^{-5}M) until a plateau was reached. Vessels were then washed, and this was repeated at least three times in order to stabilize the tissue. Endothelium-dependent and -independent relaxations were assessed by measuring the dilatory response of mesenteric arteries to cumulative concentrations of acetylcholine (from 10^{-9}M to 10^{-5}M) or nitroglycerine (from 10^{-9}M to 10^{-5}M), respectively, in vessels pre-contracted with phenylephrine at a dose necessary to obtained a similar level of pre-contraction in each ring (80% of initial KCl-evoked contraction). Some mesenteric arteries mounted on a pressure myograph were transfected with 20 μg of MMP-1 siRNA or with scrambled siRNA. In particular , siRNA was diluted into 200 μL Opti-MEM I. An equal volume of PLUS reagent was added. The mixture was incubated for 5 min. Lipofectamine LTX was added, and the complexes were allowed to form by incubation for 25 minutes[3]. Subsequently, 200 μL of complex were injected into P1-way (into vessel) of pressure myograph and then vessels were perfused at 100 mmHg for 1 hour and then at 60 mmHg for 5 hours as previously described[3].

Blood pressure Measurement

Two days before testing PTX3 on blood pressure, mice were anesthetized with 0.03 mL of a 2:1 mixture of ketamine (100 mg/mL IM, Aveco Co) and xylazine (20 mg/mL IM, Miles Inc) and placed on an operating surface maintained at 38°C. A polyethylene catheter (PE-10; Becton Dickinson, Sparks) was inserted into a femoral artery as previously described[4].

The surgery was performed in a uniform fashion by a single investigator (A.D.) between 8 AM and noon. The catheter was filled with heparinized saline solution (100 μU/ml) and exteriorized subcutaneously at the interscapular area. It was connected to a pressure transducer (WPI, TBM4M) and arterial blood pressure was monitored and recorded on a computer system (WPI, Trans Bridge 4M). After surgery, mice were individually housed in cages and allowed to recover. Direct

intrafemoral arterial pressure was measured in conscious, freely moving mice after an overnight fast as previously described[4].

Intra-arterial blood pressure was evaluated in WT and P-selectin KO mice under basal conditions and after PTX3 injection (100µg, intraperitoneally). Mice used as controls were treated in a similar way, but with PTX3 substituted with the vehicle alone. Basal blood pressure was evaluated also in WT and PTX3 KO mice for one week. At the end of blood pressure measurements, some vessels were excised for vascular reactivity, western blot or morphological analyses.

Immunoprecipitation. Mesenteric artery homogenates were prepared in 5 mM Tris-HCl buffer, pH 7.5, containing 1 mM $CaCl_2$, 1 mM $MgCl_2$, and 1 mM $NaHCO_3$. Samples containing 1 mg of total protein were lysed for 40 min at +4°C with lysis buffer at pH 7.5 containing 50 mM Tris-HCl, 150 mM NaCl, 1% NP-40, 1 mM $Na_2P_2O_7$, 1 mM NaF, 1 mM EDTA, 2 mM $NaVO_4$, 0.1 mM PMSF, and complete protease inhibitor cocktail (Roche), and centrifuged for 15 min at 20,000 g at 4°C. Supernatants were cleared with protein A/G–agarose beads (Santa Cruz Biotechnology, Inc.) for 2 hours at 4° and incubated or with anti P-selectin or with anti-Caveolin-1 antibody, followed by precipitation with protein A/G–agarose beads for 1 hour at 4°C. The beads were washed three times with lysis buffer and two times with PBS, and then analyzed by immunoblotting.

Gel electrophoresis and immunoblotting. Protein extraction was performed from four pooled mesenteric arteries. Proteins were separated on 10% SDS-PAGE and electroblotted onto nitrocellulose transfer membrane (Amersham) for 1.5h at 250 mA. Immunoblots were incubated with the appropriate primary antibodies, followed by incubation with HRP-labeled secondary antibodies, and visualized using ECL prime (Amersham & Co.). Molecular mass markers were prestained protein standards obtained from Bio-Rad laboratories. For quantitative comparisons of chemiluminescence between the lanes, the same amounts of total protein or equal amounts of immunoprecipitate were loaded in each lane. All preparations were performed three times. Values

of all experiments were used to calculate mean values and standard deviation. The chemiluminescence quantification was performed using ImageJ software. Group comparisons were made by paired *t* test.

Low temperature SDS-PAGE.

Low-temperature SDS-PAGE (LT-PAGE) was performed for detection of SDS-resistant eNOS dimer and monomer, as described previously[5].

Cell cultures. HUVEC (Lonza) were cultured in EBM-2 media (Lonza). HUVEC were cultured at 37°C in 5% CO_2/95% air by standard methodologies in 25-cm^2 T tissue culture flasks (50 ml capacity) (Falcon, Becton Dickinson Labware) in the presence of endothelial cell growth supplement. In general, HUVEC were used for our experiments after 3–5 passages. For starvation experiments, serum- and growth factor-free medium was used. For siRNA-mediated gene knockdown, HUVECs were grown to 60% to 70% confluence and transfected with Lipofectamine LTX (Invitrogen) according to the protocol of the manufacturer. As control, a scrambled-RNA was used. 24 h after siRNA transfection, cells were washed with PBS and then left for 2h in serum- and growth factor-free medium before of each treatment.

Measurement of MMP-1 activity.

HUVEC were cultured at 37°C in 5% CO2/95% air by standard methodologies in 100 mm dishes to achieve 70–80% of confluence. Treatment with PTX3 (2 and 20 ng/mL) and P-Selectin (50 and 100 ng/mL) was performed in serum- and growth factor-free medium. Cells were treated for 1 hour; at the end of treatments, medium was collected and concentrated 10X using Ultra-Amicon 10K (Sigma). MMP-1 activity was measured with a TECAN Infinite 200PRO, using SensoLyte® Plus 520 MMP-1 Assay Kit *Fluorimetric and Enhanced Selectivity* (Anaspec) by monitoring at excitation/emission wavelengths 490 nm/520 nm at the end-point, following the manufacturer's protocol.

Measurement of NO

Total NO content in the supernatants of HUVEC cultures was measured in an additional experiment. Cells were grown in 100mm dishes and supernatants collected after stimulation with acetylcholine (100 μM for 20 minutes), used to induce NO production. In some experiments, cells were pretreated with PTX3 (20ng/mL) or with siRNA MMP1 plus PTX3 (20ng/mL). The nitric oxide concentrations in the supernatant was assayed as nitrite, the stable breakdown product of NO, by a chemiluminescence detector (Sievers 280i NO Analyzer), as previously described[6].

Transmission Electron Microscopy (TEM). HUVEC pellets and mesenteric artery from control and KO mice (5 mm^3 samples) were processed for ultrastructural analysis at transmission electron microscopy by fixing in 2% paraformaldehyde and 0.1% glutaraldehyde in 0.1 M PBS, pH 7.4, for 90 min; after washing in PBS, samples were post-fixed in 1% OsO_4 for 2 hours at 4°C. Then, samples were dehydrated in ethyl alcohol and embedded in Epon–araldite. Ultrathin sections (50 nm thin) were stained with uranyl acetate and lead citrate and finally examined under an Jeol Jem 100SX transmission electron microscope (Jeol, Tokyo, Japan).

For immunocytochemistry, mesenteric arteries were processed as described for plain TEM. Post-embedding immunoelectron microscopy was performed. Ultra-thin sections (50 nm) were de-osmicated with aqueous solution of sodium metaperiodate and incubated for 24 h at 4°C with primary antibodies against CAV-1 or MMP1 (Sigma-Aldrich) diluted 1:10 in PBS containing 0.2% saponin (Sigma) and 1% normal goat serum. Then, sections were incubated with gold-conjugated secondary antibodies (20-nm gold particles) diluted 1:10 in buffer solution for 1 h at 25°C. Finally, sections were fixed with 1% glutaraldehyde, stained with uranyl acetate and lead citrate, and examined under a Jeol JEM SX 100 electron microscope. Control sections were obtained by omitting the primary antibody and incubating with only the secondary antibody.

Evans blue Dye

Vascular structure alterations on mesenteric arteries were assessed also using Evans Blue Dye (Sigma) according to the method previously described with minor modification[7]. Briefly, 50 mL of

solution containing 2% Evans blue diluted in saline was injected into the tail vein 10 minutes before euthanasia, followed by fixation with a perfusion of 4% paraformaldehyde for 10 minutes. Images were captured with an LSM 510 microscope (Carl Zeiss MicroImaging).

Immunofluorescence analysis.

On vessels:

Mesenteric arteries were treated with biotinylated PTX3 (20ng/mL) for 45 minutes and then cryopreserved in killik medium (Bioptica). Vessels were then processed in a cryostat to obtain 10-μm sections disposed on polarized slides (Carlo Erba). Sections were then extensively washed and treated with fluorescence streptavidin (1:500) and incubated for 2 hours at room temperature. Different sections of mesenteric arteries from WT and P-selectin KO mice were processed with different primary antibodies (CD31, α-SMA) to evaluate the integrity of endothelial or smooth muscular layer, and then with respective secondary antibodies. Finally, the sections were visualized with a Zeiss 2 fluorescence microscope.

Another experimental series of vessels was processed for immunohistochemical staining on 10 μm sections of cryopreserved mouse mesenteric artery in order to evaluate F4-80 expression, a well-characterized macrophage marker. All slides were stained at same time. Mesenteric arteries treated with LPS was considered as positive control. The slides were rinsed with TBS and the endogenous peroxidase inactivated with 3% hydrogen peroxide. After protein block with BSA (5% in PBS 1), the sections were incubated for one hour with antibody against F4-80 (NBPB2-12506 Rabbit Ab, Novus Biologicals, diluted 1: 20). The sections were rinsed in TBS and incubated for 20 minutes with Novocastra biotinylated secondary antibody (RE7103), a biotin-conjugated secondary antibody formulation that recognizes mouse and rabbit immunoglobulines. Then, the sections were rinsed in TBS and incubated for 20 minutes with Novocastra Streptavidin-HRP (RE7104). The peroxidase reactivity was visualized using a 3,3'-diaminobenzideine (DAB). Finally, the sections were counterstained with hematoxylin and mounted. Results were interpreted using a light

microscope LSM 510 (Carl Zeiss MicroImaging). Immunohistochemistry expression was evaluated by a pathologist.

On Cells:

HUVEC were seeded on glass coverslips and treated with 20 ng/ml PTX for the indicated time. At the end of treatments, coverslips were washed in PBS, fixed 10 min in PBS–4% paraformaldehyde and incubated 30 min in PBS containing 0.5% BSA and 50 mM NH_4Cl at room temperature without any permeabilization. For the staining of P-selectin and PTX3, coverslips were incubated for 1 hour at room temperature with 10 µg/ml mouse anti-human CD62P (BD Biosciences) and/or 20 µg/ml PTX3-specific rabbit polyclonal antibody (Sigma-Aldrich). Alexa 594- and Alexa 488-coniugated secondary antibodies (Jackson Immunoresearch) were used. The staining of CD31 was performed for 1 hour at room temperature with a 1:25 dilution of rat polyclonal CD31 specific antibody. Biotinylated anti-rat secondary antibody and Alexa 488-labelled streptavidin were used. Coverslips were mounted with the Prolong AntiFade kit. Images were collected with a laser scanning confocal microscope (LSM 510; Carl Zeiss MicroImaging) equipped with a plan Apo 63X, NA 1.4 oil immersion objective lens.

Colocalization measurements. Per cent colocalization of the fluorescence signals was quantified on a minimum of 30 different cells. 8-bit thresholded images were analyzed for Manders colocalizing coefficients with the LSM 510 4.0 SP2 software. The per cent colocalization is relative to the in-focus z-plane stack shown in the immunofluorescence panels.

Flow cytometric analysis. HUVEC were treated with PTX3 (20 ng/ml) or vehicle for 2 hours and then incubated with anti-P-selectin antibody (Santa Cruz) (diluted 1/25 in PBS) for 30 minutes at 4° C. Cells were then washed with PBS and stained with PE-conjugated goat anti-mouse IgG (Sigma-Aldrich) (diluted 1/100 in PBS) for 30 minutes at 4°C, and then followed by PBS washes. Flow cytometry measurements were performed with a FACSCanto (Becton-Dickinson, San Diego, CA) and analyzed by Flow-Jo software (Tree Star Inc., Ashland, OR).

Human samples and ELISA. Thirty-one patients with hypertension (defined as DBP ≥90 mmHg and/or SBP ≥140 mmHg or on the basis of use of anti-hypertensive medication) and 21 healthy control subjects were recruited from a specialist center at the University of Naples Federico II, Italy. The study was approved by an institutional review committee and the subjects gave their informed consent. Clinical data from each patient were collected. Patients with lung disease, heart disease, acute or chronic inflammatory disease, recent infection, presence of neoplasia, concomitant treatment with steroids or nonsteroidal anti-inflammatory drugs, or alcoholism were excluded. Blood pressure (BP) was measured with the patient seated with the use of a validated automatic device. Three consecutive readings were recorded, and the mean was used for the analysis. Characteristics of the patients are given in Table 1.

Venous blood was collected in EDTA vacuum containers and stored at −80°C. PTX3, P-selectin and MMP-1 were then measured using a high-sensitivity, enzyme-linked immunosorbent assay (ELISA) system for human plasma. Preparation of plates and sandwich ELISA were performed according to the manufacturers' instructions for each specific kit (PTX3 Human ELISA Kit, Abnova # KA1007; CD62P P-Selectin Human ELISA Kit, abcam # ab100631; MMP1 Human ELISA Kit, abcam # ab100603).

Supplemental Results

Macroscopic evaluation of PTX3-evoked vascular changes

Our data demonstrate that the target of PTX3's vascular action is the endothelium and that it induces dysfunction of resistance vessels. To further support this data, macroscopic images of changes in vascular structure were assessed using Evans Blue Dye (EBD) staining and immunohistochemistry using labeled markers for endothelium and smooth muscle (CD31, α-SMA). We found that only PTX3-treated vessels acquired EBD (Fig. S3a) and showed a significant

reduction of CD31, indicating a specific alteration of the endothelial layer, since no differences were observed in the smooth muscle marker (Fig. S3b).

SAP induces an impairment of eNOS phosphorylation

Considering the endothelial dysfunction induced by SAP at the vascular level, we performed Western blotting on resistance vessels from WT and P-selectin deficient mice exposed to SAP, to evaluate the phosphorylation status of eNOS. Interestingly, the impairment of eNOS phosphorylation evidenced in vessels from WT mice was absent in P-selectin knockout mice (Fig S5). These data were coherent with the results on vascular reactivity.

PTX3-evoked vascular damage is not associated with macrophage recruitment

We studied the possible recruitment of immune cells in vessels from WT and P-selectin KO mice treated with PTX3. Our histologic and immunohistochemistry analyses clearly demonstrate that in both WT and P-selectin KO mice treated with PTX3, there was no positivity for F4-80, an extensively used marker for macrophage cells, compared to positive control vessels treated with LPS, in which each sections showed a well-marked cell. We conclude that PTX3-evoked vascular action is not associated with a recruitment of macrophages to the vessel wall (Fig. S6).

Effect of PTX3 on HUVEC

a) Effect of PTX3 on P-selectin expression

Confocal microscopy revealed that treatment with PTX3 (20ng/mL for 0–60 minutes) induced expression of P-selectin on cell membranes (Fig. S8a). To confirm this, we performed flow cytometry experiments, finding that exposure to exogenous PTX3 up-regulated P-selectin expression in HUVEC, as indicated by a rightward shift in the output curve (increased percentage of positive cells and higher mean fluoresce intensity) (Fig. S8b).

b) Effect of PTX3 on NO production

Western blotting revealed a significant increase of MMP-1 expression in cells treated with PTX3 (Fig. S9a). In addition, spectrofluorimetry detected a significant increase in MMP-1 activity (Fig. S9b). As observed at the vascular level, PTX3 impaired NO signaling also in isolated endothelial cells, as evidenced by reduced dimerization of eNOS and phosphorylation on serine 1177 (Fig. S9c). At the function level, PTX3 markedly decreased nitric oxide production when compared to vehicle (Fig. S9d). Inhibition of MMP-1 by siRNA MMP1 hampered PTX3's deleterious effect on nitric oxide signaling, as revealed by a complete rescue of dimerization and phosphorylation of eNOS in serine 1177, effects associated with an enhanced production of nitric oxide (Fig. S9d).

To clarify whether P-selectin, *per se*, was able to modulate MMP-1 signaling, we treated HUVEC with P-Selectin at different dosages. Although P-selectin did not change MMP-1 expression, it was able to significantly enhance its activity. This effect was lower compared to that observed in the presence of PTX3 (Fig. S9a, S9b).

Hypertensive patients have elevated plasma levels of PTX3, P-selectin and MMP-1

Univariate tests showed that PTX3 (ng/mL), P-selectin (ng/mL) and MMP-1 (pg/mL) values were significantly higher in hypertensive subjects with respect to controls ($p < 2 \times 10^{-8}$) (Table S1). It is important to underline that PTX3 was the strongest predictor of hypertension, reaching the highest *p*-value, as reported in Table S1. The second goal of the analysis was to identify the most informative threshold for each variable to discriminate hypertensive subjects from controls. To this aim, the dataset was randomly split into a *training set* (37 subjects, 70% of the whole sample) and a *test set* (15 subjects, the remaining 30% of the data). Random sampling was performed with stratification, so that the proportion of cases and controls observed in the whole sample (60% *vs*. 40%) was maintained also in the two sub-cohorts. Thus, the *training set* was used to identify the most discriminative threshold for each variable, as described in Methods Section. The *test set* was then used to evaluate the discriminative performances corresponding to the variables discretized according to the identified threshold. Results are reported in Table S2 and show that PTX3

discretized according the threshold corresponding to ≥ 2.508 reaches the highest MCC, sensitivity and F-Measure among the analysed variables.

Supplemental Figures and Figure Legends.

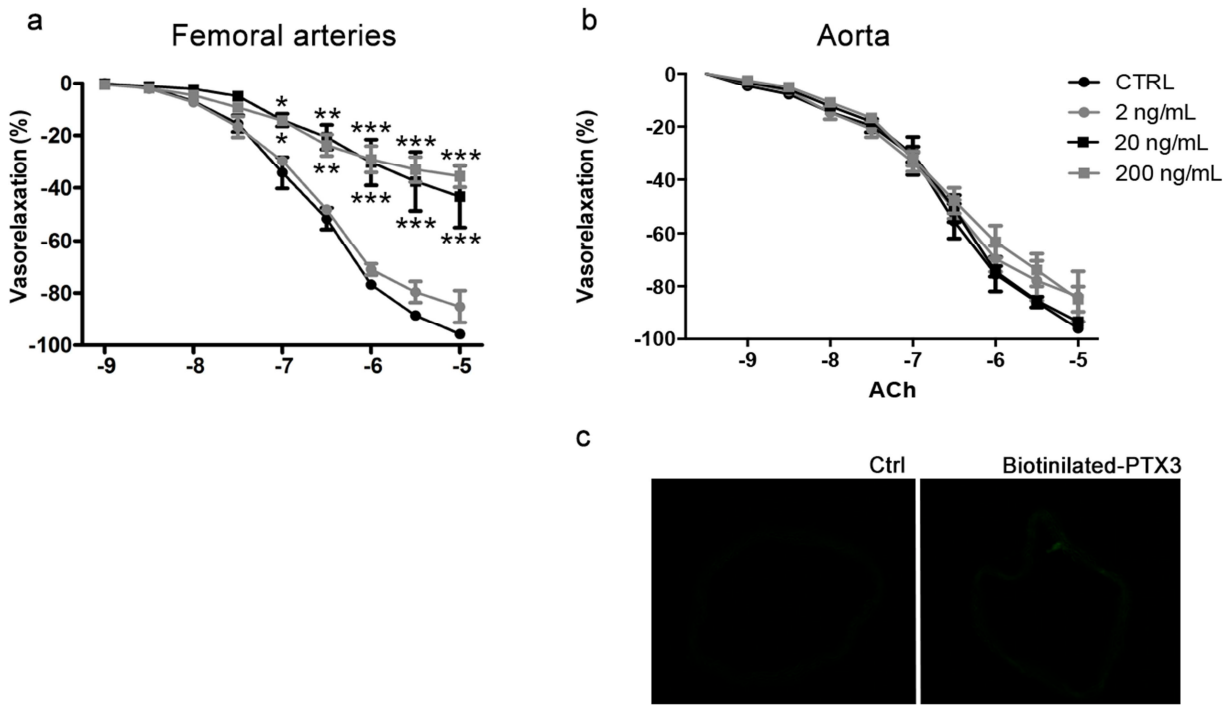

Figure S1. Effects of PTX3 on femoral arteries and aorta. **a)** Dose–response curves of phenylephrine-precontracted femoral arteries from C57BL/6N mice to acetylcholine after 45 minutes of PTX3 treatment at different dosage (2, 20, 200 ng/mL). **b)** Dose–response curves of phenylephrine-precontracted aorta rings from C57BL/6N mice to acetylcholine after 45 minutes of PTX3 treatments at different dosage (2, 20, 200 ng/mL). *, $p<0.05$; **, $p<0.001$; ***, $p<0.0001$ vs control or 2 ng/mL. (n=8 both for femoral arteries and aorta. **c)** Immunohistochemical staining, using fluorescent streptavidin, of aorta sections from C57BL/6N mice treated with vehicle or with biotinylated-PTX3. Scale bar, 100 µm. (n=4)

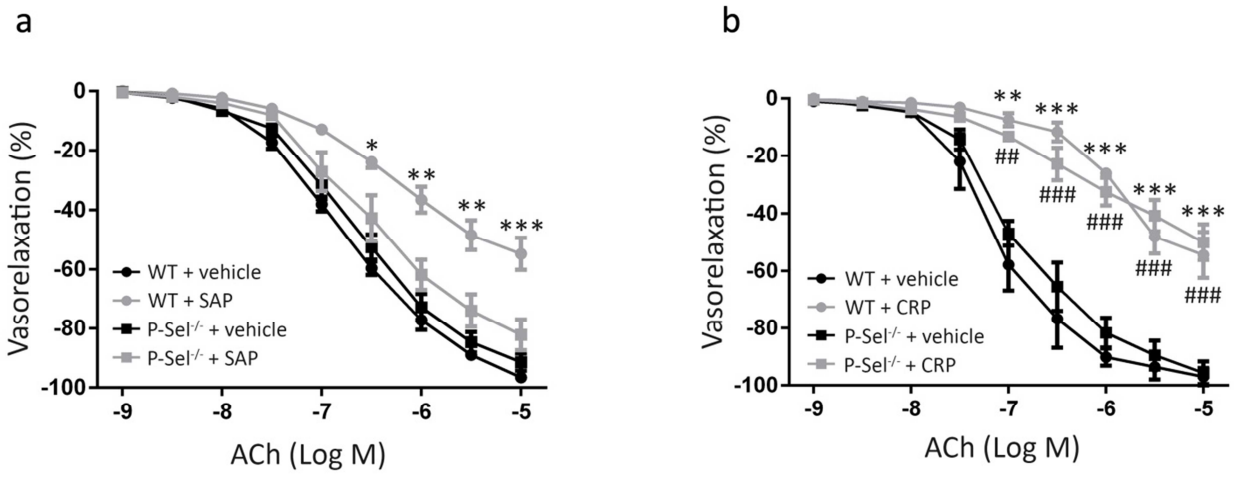

Figures S2. a) Dose–response curves to acetylcholine (Ach) in phenylephrine-precontracted mesenteric arteries from wild-type (WT) and P-Selectin KO (P-sel$^{-/-}$) mice: vessels were exposed to vehicle alone or to SAP for 45 minutes (200ng/mL); n=4 for each group. **b)** Dose–response curves to Ach of phenylephrine-precontracted mesenteric arteries from WT and P-Selectin KO mice: vessels were exposed to vehicle only or to CRP for 45 minutes (25µg/mL) n=4 for each group. ***, $p<0.0001$ vs WT. ###, $p<0.0001$ vs WT.

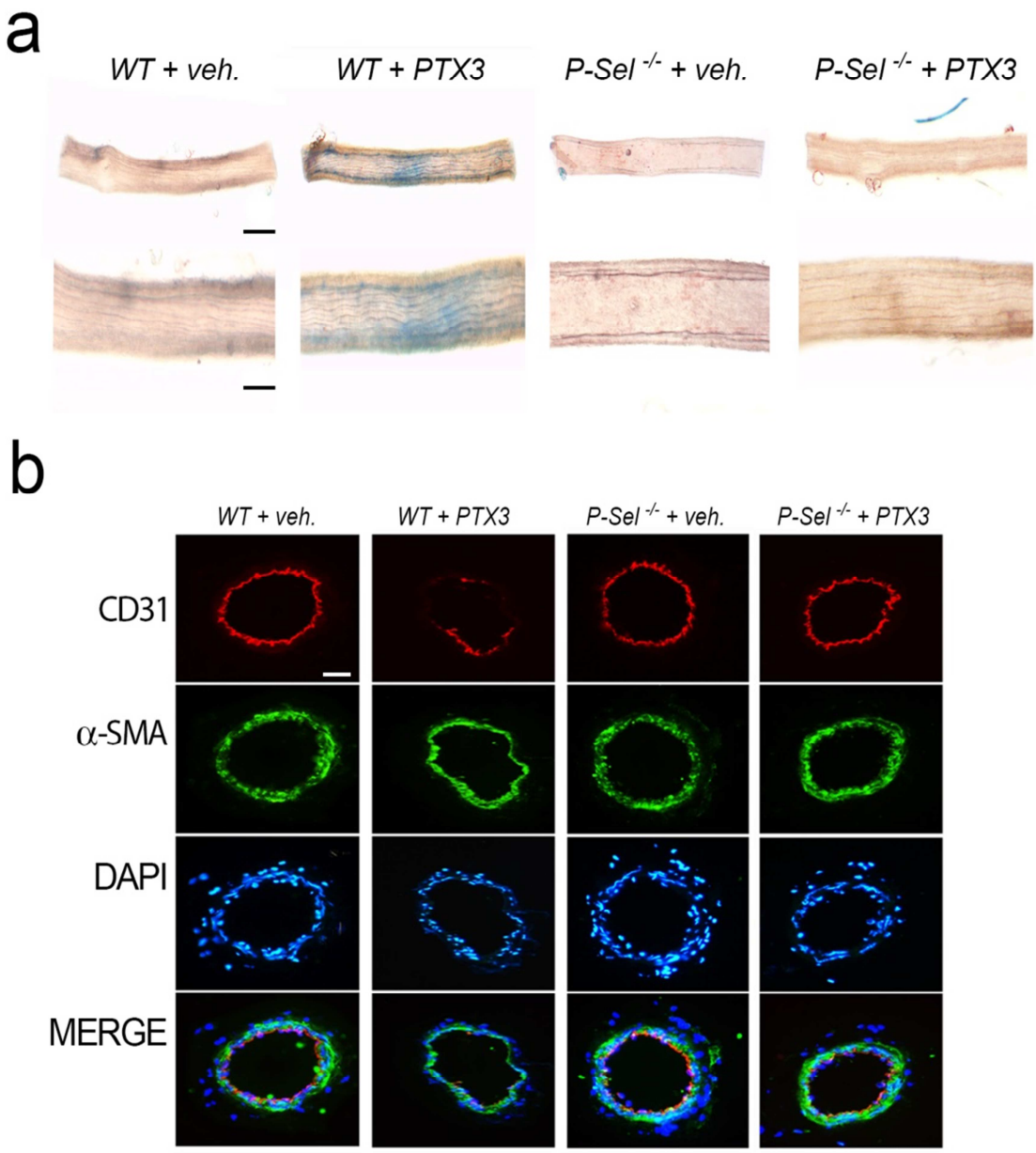

Figure S3. a) Representative images of Evans blue staining in mesenteric artery from WT and P-Selectin KO mice treated with vehicle or with PTX3. (n=3 for each group); **b)** Immunohistochemical staining of mesenteric arteries from WT and P-Selectin KO mice using a labeled endothelial marker, CD31 or a labeled smooth muscle marker, α-SMA. DAPI was used to stain nuclei. Scale bar 100 µm. (n=3 for each group).

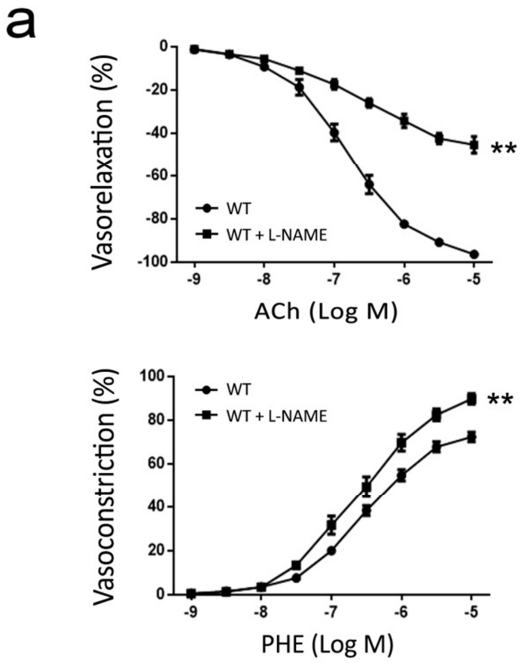

Figure S4. a) Dose–response curves to acetylcholine (Ach) (*upper*) or to phenylephrine (*bottom*) in mesenteric arteries from wild-type mice in the basal condition and after exposure to L-NAME (300 μM). **, $p<0.001$ vs WT; n=4 for each group.

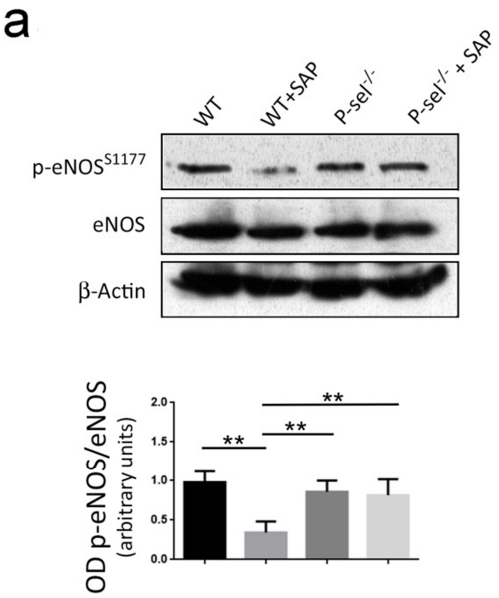

Figures S5. a) Representative Western blots for p-eNOS on serine 1177 in mesenteric arteries from WT and P-selectin KO mice exposed to vehicle or to SAP. *Bottom:* Densitometric analyses of 3 independent experiments. *, $p<0.05$. (n=3).

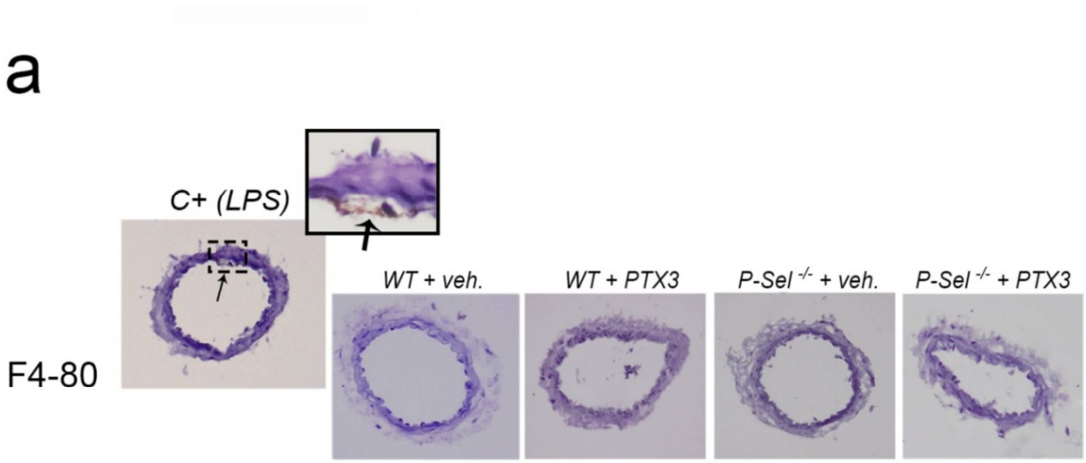

Figure S6. a) Histologic and immunohistochemistry analyses of F4-80 expression in mouse mesenteric arteries; positive F4-80 cytoplasmic expression was found only in LPS-treated vessel (C+), while WT and P-selectin KO mice vessels, treated with vehicle or with PTX3, were negative for the macrophage marker (n=3). Scale bar 100 µm.

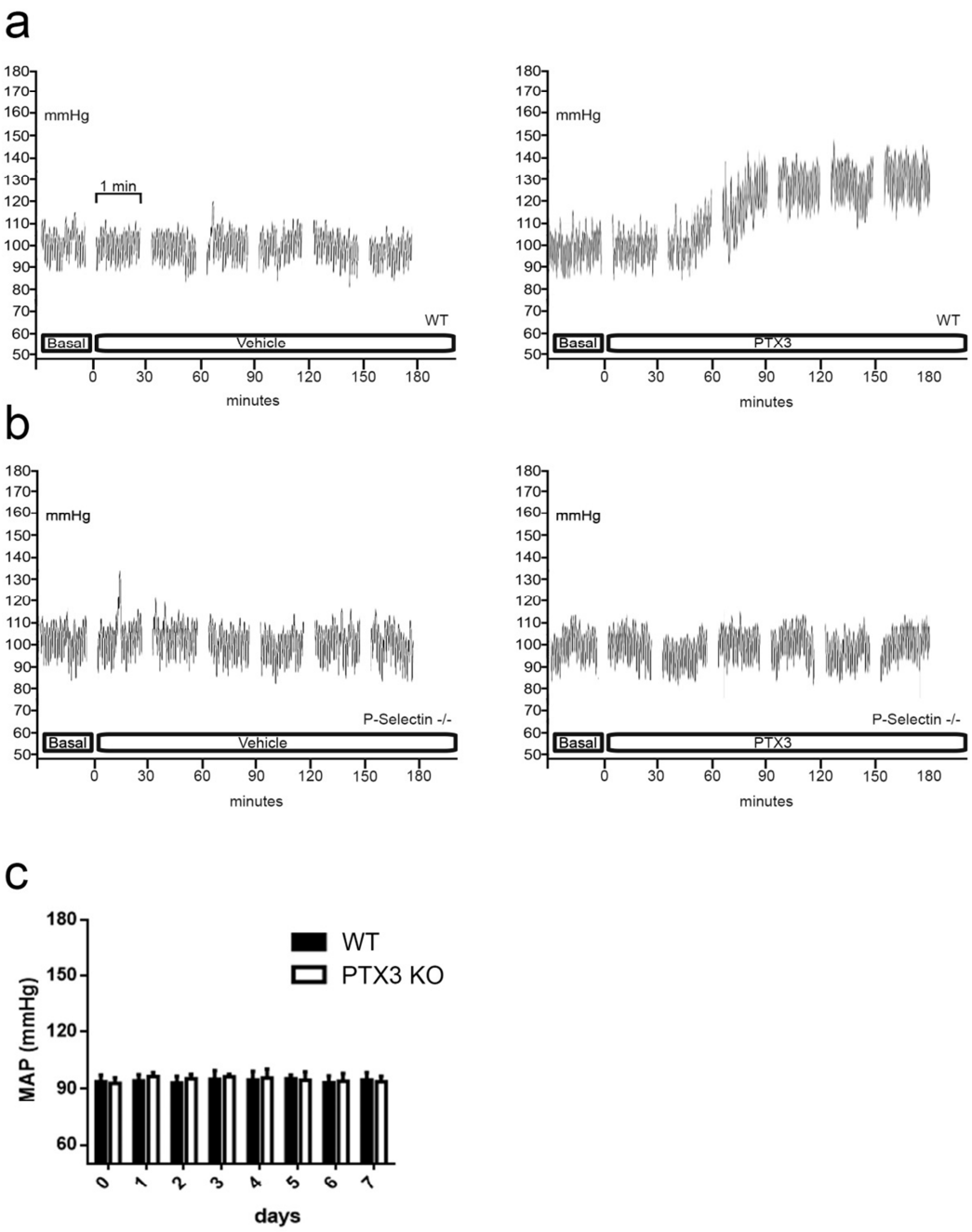

Figure S7. Representative original traces obtained during the measurement of blood pressure with a catheter injected into mouse femoral arteries. **a)** Graphs of the effects on blood pressure in wild-type mice after injection with vehicle (*left*) or with PTX3 *(right)*. **b)** Graphs of the effects on blood pressure in P-selectin knockout mice (P-selectin$^{-/-}$) after injection with vehicle (*left*) or with PTX3 *(right)*. **c)** Mean arterial pressure (MAP) measured by indwelling femoral catheters in WT and PTX3-knockout mice; n=5 for each group.

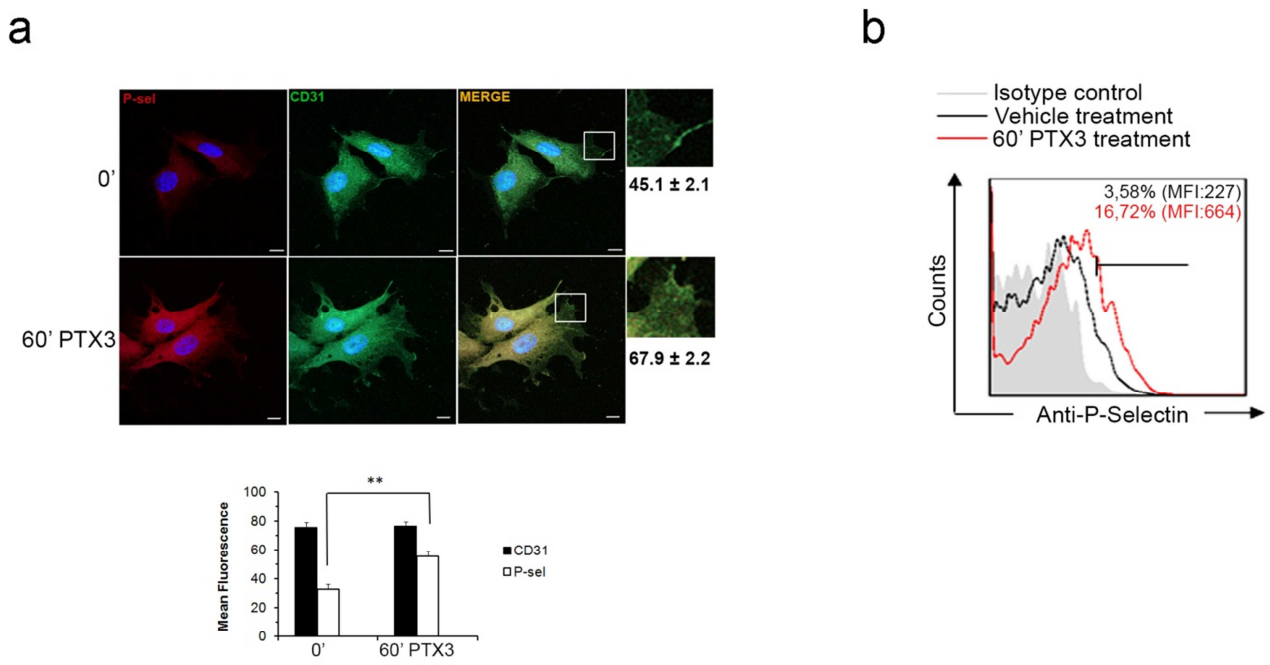

Figure S8. a) HUVEC seeded on glass coverslips were either untreated (0 minutes) or treated for 60 minutes with PTX3 (20ng/mL). Colocalization is shown in yellow in the merged panels, and quantified as Manders colocalizing coefficients in the histogram below. $^{**}p<0.05$. Cells were processed for immunofluorescence with P-selectin (P-sel) and CD-31 (a membrane-specific) antibodies; n=4. **b)** Cytofluorimetric analysis of HUVEC treated for 1 hour with 20ng /mL PTX3. The plot gives the increment as a percentage of P-selectin on the membrane of the human endothelial cells; n=4. MFI, mean fluorescence intensity.

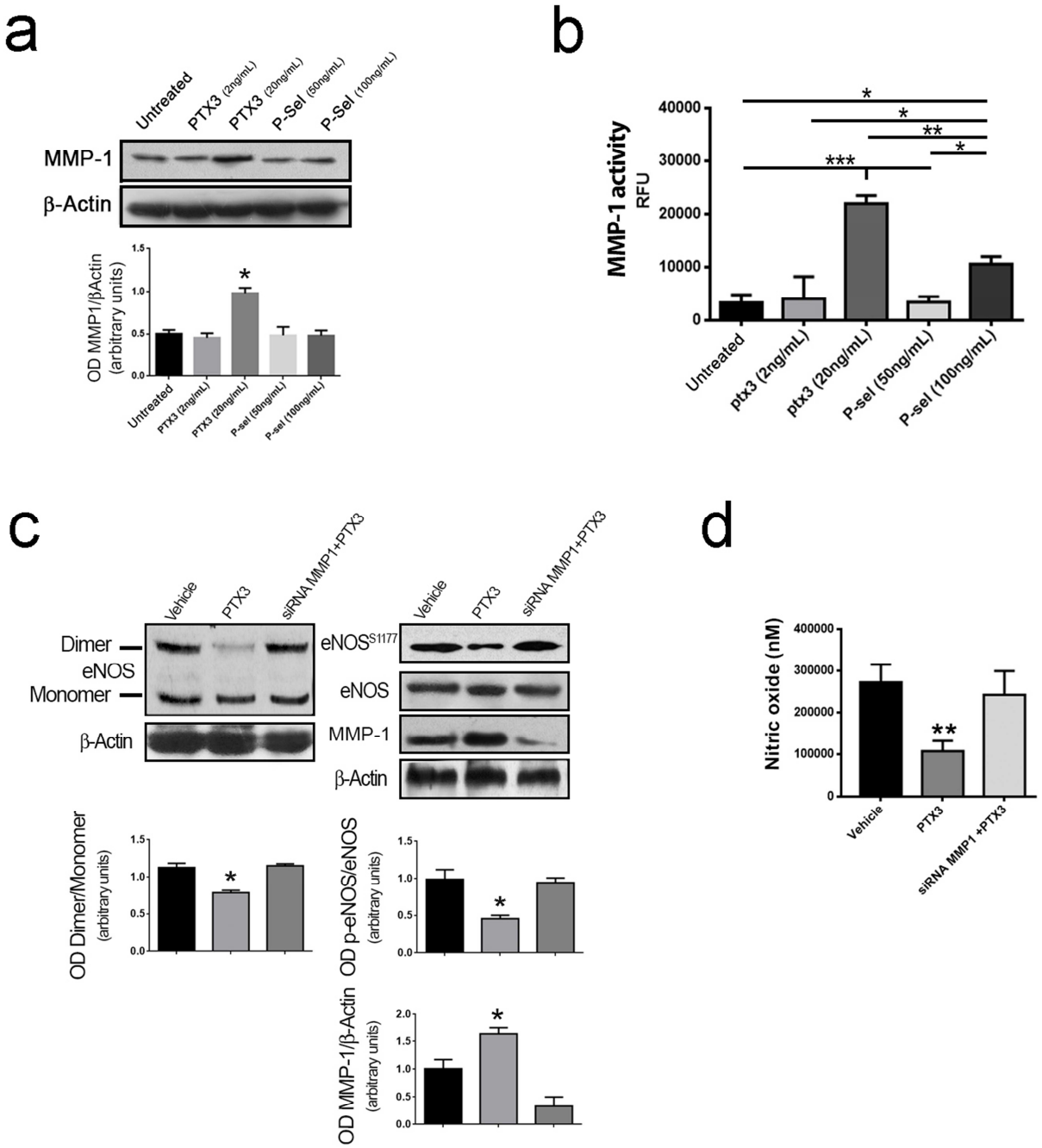

Figure S9. a) *Upper*: representative Western blots for MMP-1 expression in HUVEC without treatment (untreated), treated for 1 hour with PTX3 (2 or 20ng/mL) or with P-selectin (50 or 100ng/mL). *Bottom*: Densitometric analyses of 3 independent experiments. *, p<0.05. **b)** MMP1 activity measured in HUVEC without treatment (untreated), treated for 1 hour with PTX3 (2 or 20ng/mL) or with P-selectin (50 or 100ng/mL). Data of 3 independent experiments. *, p<0.05; **, *p*<0.001; ***, *p*<0.0001. **c)** representative Western blots for eNOS monomers/dimers (*left*) and for

p-eNOS on serine 1177 (*right*) in HUVEC treated with vehicle, with PTX3, or with PTX3 after siRNA MMP1 transfection. All cells were stimulated with acetylcholine (100µM for 20 minutes). *Bottom*: Densitometric analyses of 3 independent experiments. *, $p<0.05$. **d)** NO measured in supernatants of HUVEC treated with vehicle, with PTX3, or with PTX3 after siRNA MMP1 transfection. All cells were stimulated with acetylcholine (100µM). Data are mean±SEM of 3 independent experiments. **, $p<0.01$).

Supplemental Tables.

Table S1. **Discriminative performances of the analyzed variables**.

Variable	Hypertensive	Control	p-value	AUROC (95% CI)
PTX3 (ng/mL)	3.36 (2.74-4.69)	1.44 (1.11-2.03)	4.01×10^{-9}	0.985 (0.963-1)
SEL-P (ng/mL)	69.68 ± 11.47	48.84 ± 9.85	8.08×10^{-9}	0.919 (0.850-0.989)
MMP-1 (pg/mL)	301.7 (239.9-369.86)	96.25 (78.22-123.66)	1.59×10^{-8}	0.966 (0.927-1)

Variable, analyzed variable; Hypertensive, mean ± SD or median (25th-75th percentiles) of each variable's distribution in hypertensive subjects (n = 31); Control, mean ± SD or median (25th-75th percentiles) of each variable's distribution in control subjects (n = 21); p-value, probability value deriving from the Welch's t-test or Wilcoxon rank-sum test as appropriate; AUROC, Area Under the Receiver Operating Characteristic curve and corresponding 95% Confidence Interval (CI).

Table S2. **Discriminative performances of the analyzed variables discretized according to the identified thresholds.**

Variable	Threshold	Set	MCC	Sens.	Spec.	PPV	NPV	F
PTX3	≥ 2.508 ng/mL	Training	0.850	0.864	1.000	1.000	1.000	0.927
		Test	1.000	1.000	1.000	1.000	1.000	1.000
SEL-P	≥ 56.333 ng/mL	Training	0.660	0.909	0.733	0.833	0.833	0.869
		Test	0.720	0.889	0.833	0.889	0.889	0.889
MMP-1	≥ 192.028 pg/mL	Training	0.850	0.864	1.000	1.000	1.000	0.927
		Test	0.870	0.889	1.000	1.000	1.000	0.941

Variable, analysed variable; Threshold, identified threshold; set, training (22 hypertensive subjects vs. 15 controls) or test (9 hypertensive subjects vs. 6 controls) sets; MCC, Mattew's Correlation Coefficient; Sens., sensitivity; Spec., specificity; PPV, Positive Predictive Value; NPV, Negative Predictive Value; F, F-Measure.

References.

1. Bottazzi B, Vouret-Craviari V, Bastone A, De Gioia L, Matteucci C, Peri G, Spreafico F, Pausa M, D'Ettorre C, Gianazza E, Tagliabue A, Salmona M, Tedesco F, Introna M and Mantovani A. Multimer formation and ligand recognition by the long pentraxin PTX3. Similarities and differences with the short pentraxins C-reactive protein and serum amyloid P component. *J Biol Chem*. 1997;272:32817-23.

2. Zacchigna L, Vecchione C, Notte A, Cordenonsi M, Dupont S, Maretto S, Cifelli G, Ferrari A, Maffei A, Fabbro C, Braghetta P, Marino G, Selvetella G, Aretini A, Colonnese C, Bettarini U, Russo G, Soligo S, Adorno M, Bonaldo P, Volpin D, Piccolo S, Lembo G and Bressan GM. Emilin1 links TGF-beta maturation to blood pressure homeostasis. *Cell*. 2006;124:929-42.

3. Vecchione C, Carnevale D, Di Pardo A, Gentile MT, Damato A, Cocozza G, Antenucci G, Mascio G, Bettarini U, Landolfi A, Iorio L, Maffei A and Lembo G. Pressure-induced vascular oxidative stress is mediated through activation of integrin-linked kinase 1/betaPIX/Rac-1 pathway. *Hypertension*. 2009;54:1028-34.

4. Lembo G, Vecchione C, Fratta L, Marino G, Trimarco V, d'Amati G and Trimarco B. Leptin induces direct vasodilation through distinct endothelial mechanisms. *Diabetes*. 2000;49:293-7.

5. Carrizzo A, Puca A, Damato A, Marino M, Franco E, Pompeo F, Traficante A, Civitillo F, Santini L, Trimarco V and Vecchione C. Resveratrol improves vascular function in patients with hypertension and dyslipidemia by modulating NO metabolism. *Hypertension*. 2013;62:359-66.

6. Cudmore MJ, Hewett PW, Ahmad S, Wang KQ, Cai M, Al-Ani B, Fujisawa T, Ma B, Sissaoui S, Ramma W, Miller MR, Newby DE, Gu Y, Barleon B, Weich H and Ahmed A. The role of heterodimerization between VEGFR-1 and VEGFR-2 in the regulation of endothelial cell homeostasis. *Nat Commun*. 2012;3:972.

7. Lindner V, Fingerle J and Reidy MA. Mouse model of arterial injury. *Circ Res*. 1993;73:792-6.

Circulation
Journal of the American Heart Association

Pentraxin 3 Induces Vascular Endothelial Dysfunction Through a P-selectin/MMP-1 Pathway

Albino Carrizzo, Paola Lenzi, Claudio Procaccini, Antonio Damato, Francesca Biagioni, Ambrosio Mariateresa, Giusy Amodio, Paolo Remondelli, Carmine Del Giudice, Raffaele Izzo, Alberto Malovini, Luigi Formisano, Vincenzo Gigantino, Michele Madonna, Annibale A. Puca, Bruno Trimarco, Giuseppe Matarese, Francesco Fornai and Carmine Vecchione

Circulation. published online March 6, 2015;
Circulation is published by the American Heart Association, 7272 Greenville Avenue, Dallas, TX 75231

Print ISSN: 0009-7322. Online ISSN: 1524-4539